2016

Low Complex PAPR Reduction Schemes for OFDM Systems

Siyu Zhang
University of Windsor

Low Complex PAPR Reduction Schemes for OFDM Systems

by

Siyu Zhang

A Thesis

Submitted to the Faculty of Graduate Studies

through Electrical and Computer Engineering

in Partial Fulfilment of the Requirements for

the Degree of Master of Applied Science at the

University of Windsor

Windsor, Ontario, Canada

2016

Low Complex PAPR Reduction Schemes for OFDM Systems

by

Siyu Zhang

APPROVED BY:

Dr. R. Kent, Outside Reader

School of Computer Science

Dr. S. Erfani

Department of Electrical and Computer Engineering

Dr. B. Shahrrava, Advisor

Department of Electrical and Computer Engineering

May 10, 2016

AUTHORS DECLARATION OF ORIGINALITY

I hereby certify that I am the sole author of this thesis and that no part of this thesis has been published or submitted for publication.

I certify that, to the best of my knowledge, my thesis does not infringe upon anyones copyright nor violate any proprietary rights and that any ideas, techniques, quotations, or any other material from the work of other people included in my thesis, published or otherwise, are fully acknowledged in accordance with the standard referencing practices. Furthermore, to the extent that I have included copyrighted material that surpasses the bounds of fair dealing within the meaning of the Canada Copyright Act, I certify that I have obtained a written permission from the copyright owner(s) to include such material(s) in my thesis and have included copies of such copyright clearances to my appendix.

I declare that this is a true copy of my thesis, including any final revisions, as approved by my thesis committee and the Graduate Studies office, and that this thesis has not been submitted for a higher degree to any other University or Institution.

ABSTRACT

In this thesis, three low-complex PAPR reduction schemes for OFDM systems are proposed. All the proposed schemes can be considered as modified versions of the conventional SLM scheme, which can significantly reduce high PAPR of OFDM signals with no distortion.

In the first proposed scheme, a new set of the candidate sequences is generated by partial phase weighting in the time domain and the combination of sub-blocks by applying IFFT properties. In the second scheme which is based on a combination of SLM and PTS, a simple phase optimization technique is introduced. The third scheme forms different 16-QAM signals from 2 QPSK signals. Also, the circular convolution part in TPPW-SLM, which is also a part of Class-III SLM, is applied.

A comparison among the proposed schemes, in terms of PAPR reduction performance and computational complexity reduction, is made, thus allowing selection of the most suitable scheme for a given application.

DEDICATION

To my loving parents:

Father: Zhang Ruicheng

Mother: Zhao Yanping

ACKNOWLEDGEMENTS

I would like to express my sincere gratitude and appreciation to everyone who helped make this thesis possible. First of all, I would appreciate my parents. Their support encouraged me to overcome all difficulties that I met during my study. They supported me to study aboard and gave me financial support, without whom, I could not achieve my study. Also, I am deeply indebted to my supervisor Dr. Behnam Shahrrava, professor of Electrical and Computer Engineering at University of Windsor, for guiding me throughout the writing of this thesis. As one of best teachers I have ever had, Dr. Shahrrava impressed upon me that a good teacher instructs students in matters far beyond those in textbooks. His broad knowledge and logical way of thinking have been of great value; without his detailed and constructive comments on my research, none of this thesis would be possible. Dr.R. Kent from the School of Computer Science also gave me a lot of help. He read through my thesis page by page and gave me advice about how to use words in technical writing. I really appreciate it.

I would also grateful to my colleagues and friends, Chen Chen, Ruiqing Dong, Bingxin Liu and Philip Ugbaja and Chunyu Mao, who gave me their help and time in listening to me and helping me work out my problems during the difficult course of the thesis.

Finally, I wish to extend my gratitude to the faculties of Electrical and Computer Engineering at University of Windsor for their efforts and help during my study for the master degree. Moreover, my thanks would go to the financial support from the University of Windsor and my supervisor Dr. Behnam Shahrrava.

Siyu Zhang

TABLE OF CONTENTS

LIST OF TABLES

LIST OF FIGURES

LIST OF ACRONYMS

ACE active constellation extension

ADC analog to digital convertor

ADSL asymmetric digital subscriber line

API average power increase

BER bit error rate

CC computational complexity

CCDF complementary cumulative distribution function

CDMA code-division multiple access

CP cyclic prefix

DAB digital audio broadcasting

DFT discrete fourier transform

DIF differential item functioning

DRL data rate loss

DSP digital signal processing

DVB digital video broadcasting

FFT fast fourier transform

GI guard interval

HDSL high-bit-rate digital subcriber line

HPA high power amplifier

ICI inter-carrier interference

IDFT inverse discrete fourier transform

IFFT inverse fast fourier transform

ISI inter-symbol interference

LO local oscillator

LTE long term evolution

MC multi-carriers

OBR out-of-band radiation

OFDM orthogonal frequency division multiplexing

PAPR peak to average power ratio

PBISLM partial bit inverted SLM

PPPW-SLM partitioning and partial-phase-weighting-SLM

PRC PAPR reduction capabilitiy

PRT peak reduction tone

PTS orthogonal frequency division multiple access

PTS partial transmit sequence

PTS partial transmit sequence

QAM quadrature amplitude modulation

QPSK quadrature phase shift keying

RF radio requency

RMS root mean square

SC single-carrier

SC-FDMA single carrier frequency division multiple access

SI side information

SLM selected mapping

SNR signal-to-noise ratio

SSPA solid state power amplifier

TI tone injection

TPPW-SLM time-domain-partial-phase-weighting-SLM

TR tone resercation

TWTA traveling wave tube amplifier

VC variance of correlation

WLAN wireless local area networks

WMAN wireless local and metropolitan area networks

1 INTRODUCTION

1.1 The development of OFDM and its applications

OFDM is a special multi-carrier modulation (MCM) technique. The main idea of OFDM is to divide a high speed data stream into several low speed data streams and modulate on subcarriers that are orthogonal with each other. In this way, OFDM makes the symbol period longer than the delay spread, which avoids the small scale fading and intersymbol interference (ISI) [1]. Moreover, OFDM is spectrally very efficient since the subcarriers have significant overlap in the frequency domain [2].

1.1.1 The development of OFDM

The concept of OFDM techniques was first proposed by R. W. Chang in 1965 [3]. OFDM is a special case of the frequency division multiplexing (FDM), which is used by the American National Defense Department for military communications. Compared with the conventional FDM, OFDM allows the spectrums from different subcarriers that are orthogonal to be overlapped with each other, which improves the spectral efficiency of the system. In 1967, Saltzberg analyzed the performance of OFDM systems [4]. The OFDM technology was patented in 1970 at the USPD [5], and was used in high-frequency military communication systems in the 1970s.

In 1971, S. B. Weinstern and P. M. Ebert employed the discrete fourier transform (DFT) into the MCM [6]. In practice, the fast fourier transform (FFT) implementation of the DFT has made OFDM modulation and demodulation feasible and very successful. In the 1980s, Peled and Ruiz [7] inserted cyclic prefix (CP) into OFDM signals to guarantee the orthogonality among subcarriers, which dramatically decreased the ISI caused by a multi-path channel.

1.1.2 The applications of OFDM

OFDM is less sensitive to frequency selective fading, and transmit high-speed data with higher spectral efficiency. Thus, more and more people have been focusing on OFDM. OFDM has been widely used in wideband communication systems since the 1990s, such as digital audio broadcasting (DAB) [8], high-bit-rate digital subscribe line (HDSL) [9], asymmetric digital subscriber line (ADSL) [10]. Currently, OFDM is the core technique of wireless local area networks (WLAN) [11], wireless local and metropolitan area networks (WMAN), [12] and [13], and 4G-LTE networks.

In 1995, the European Telecommunication Standards Institute (ETSI) adopted the DAB standard, which is the first standard that deployed OFDM. In 1997, the standard of digital video broadcasting (DVB) based on OFDM was adopted. OFDM was used in wireline applications successfully such as ADSL, which can provide at most $8M$bit/s data rate in $1M$Hz bandwidth. In 1997, IEEE802.11 group selected OFDM as the access scheme of physical layer (PHY) in WLAN, which aims at providing 6 Mbits/s up to 54 Mbit/s data rate. In 2001, IEEE802.16 also selected OFDM in WMAN because of the advantages of OFDM.

Furthermore, OFDM is easy to be combined with other techniques, such as space-time coding (STC), multiple input multiple output (MIMO), adaptive resource allocation, adaptive coding, which can further improve the reliability of communication systems. In this way, the interference, including ISI and ICI, can be further eliminated and the system performance can be improved.

1.2 Research background

1.2.1 Advantages an disadvantages of OFDM

Compared with single carrier modulation systems, OFDM has a number of advantages, which caused OFDM to replace CDMA techniques in 4G LTE networks. The

main advantages are listed as follows, [2] and [14]:

- **Robustness against narrowband cochannel interference**: An OFDM system can perform very well in frequency selective fading channels. For single carrier modulation, the receiver needs to use a very complex equalizer to compensate the effect caused by frequency selective fading. However, since OFDM converts a high-speed data stream into many low-speed data streams that are modulated on subcarriers, each subcarrier undergoes a flat fading. As a result, equalization is very simple in OFDM and can be easily deployed by only a single-tap equalizer for each subcarrier. Thus, OFDM is suitable for severe channel conditions without complex time-domain equalization. Although some subcarriers may suffer serious fading, this problem can be solved by coding and interleaving techniques.

- **Robustness against ISI and fading caused by multipath propagation**: OFDM is more resistant to time-varying fading due to multipath propagation. When the symbol period becomes longer (by splitting high speed serial data up to low speed parallel data), the corresponding effect caused by time-varying fading will decrease proportionally. Hence, the sensitivity of OFDM to time synchronization errors is very low. Furthermore, the ISI and ICI can be completely eliminated by introducing CP or guard interval (GI).

- **High spectral efficiency**: OFDM has very high spectral efficiency by allowing overlapping among the subcarriers compared with other modulation schemes. The conventional guard-bands in FDM can be eliminated by OFDM by making use of the orthogonality among subcarriers. The bandwidth can be saved and frequency resources can be used more effectively by using overlapped subcarriers.

- **Simple implementation using FFT/IFFT**: OFDM has effective and simple

modulation and demodulation process. The modulation and demodulation of OFDM can be implemented by IFFT and FFT, which do not need very stable high-frequency oscillators.

- **Frequency diversity**: OFDM has inherent frequency diversity, which helps OFDM cope with frequency selective fading.

However, OFDM also has some obstacles that need to be overcome in the implementation of OFDM systems:

- **Sensitivity to carrier offset and drift**: OFDM is sensitive to frequency synchronization problems. Because OFDM has a high requirement for the orthogonality among subcarriers, a little phase noise and frequency offset will impair the orthogonality among sub-carriers, which causes bit-error-rate (BER) performance degradation.

- **High peak to average power ratio (PAPR)**: Most multicarrier modulation schemes (such as OFDM) have high PAPR compared with single carrier systems. Since there are enough subcarriers with the same phase, the instantaneous amplitude caused by those overlapped signals will be much larger than the mean power of the sub-carriers, which causes high PAPR. The high PAPR requires radio frequency (RF) amplifiers to have a large dynamic range, which wastes the resources of amplifiers and decreases the corresponding efficiency. Moreover, if the instantaneous power exceeds the linear region, those signals will be distorted, which causes out-of-band radiation and BER degradation.

In order to use the OFDM technique in practice, these drawbacks need to be restrained or compensated. This thesis is concerned with developing techniques for reducing PAPR and addressing the relevant implementation issues.

1.2.2 Current research on PAPR reduction

High PAPR has become a critical problem that needs to be solved in an OFDM system. The envelope of a an OFDM is not constant. Occasionally, a large signal peak can occur when many subcarriers are added in phase. OFDM signals with high PAPR when transmitted through a nonlinear device, such as a high power amplifier (HPA), can suffer intermodulation distortion and out-of-band emission (spectral regrowth). The first effect degrades the BER performance of the system while the latter effect causes interference to other users and thus decreases the cellular capacity of the system.

Developing an algorithm to reduce PAPR has become a popular field since the 1990s, and is becoming much more popular with the 4G applications. Many institutions and universities make this problem the focus of their research.

Currently, the on-going approaches for reducing PAPR can be generally divided into three categories [15]: limiting class, signal scrambling, and encoding approaches. The limiting class approach is the most straightforward method for PAPR reduction. At the transmitter, those signals whose peak are larger than a threshold are clipped before being sent into the digital-to-analog coveter (DAC) or the radio -frequency (RF) power amplifier. The scrambling approach is different from the limiting one, since it does not clip signals, but it decreases the probability that high PAPR signals can occur. The scrambling technologies try to represent a data sequence by different sequences. In this way, the systems can pick one sequence that has the lowest PAPR for transmission. The encoding approach encodes a signal by confining the code sets and select those that are less than a threshold for transmission.

However, the evaluation criteria for a PAPR reduction algorithm are not limited to PAPR reduction performance. There are many factors that must be considered. Some PAPR reduction techniques can effectively reduce PAPR but they are too complex to be realized; this confines the use of them in practice. A technique can be simple

and easy to implement; however, its PAPR reduction performance may not be as good as that of other techniques. Hence, both PAPR reduction performance and computational complexity need to be considered and a trade-off between them need to be made.

1.3 The scope and organization of the thesis

This thesis mainly focus on PAPR reduction schemes. Many researchers have proposed a variety of PAPR reduction schemes; however, the thesis mainly focus on the selective mapping] (SLM) scheme, which has efficient PAPR performance. The main research direction is how to decrease the computational complexity of the SLM scheme while keeping a comparatively effective PAPR reduction performance. In this thesis, three PAPR reduction schemes are proposed that can be considered as low-complex modified versions of the conventional SLM scheme. First, a time domain partial phase weighting SLM (TPPW-SLM) scheme by making use of the properties of IFFT and circular convolution is proposed. Then, a combination of SLM schemes with PTS schemes while keeping a comparatively low computational complexity is presented. Finally, a low-complex SLM scheme based on QAM signals is proposed, which constructs different high-order 16-QAM signals by using low-order QPSK signals in order to generate different candidate sequences in the SLM scheme. The outline of this thesis is as follows:

In chapter 2, some background fundamentals about OFDM systems are presented and a brief introduction of vital techniques in OFDM systems are given. In chapter 3, the high PAPR issue in OFDM systems is introduced, which contains the generation, definition, and probability distribution of PAPR. Then, some popular and classical PAPR reduction techniques are presented, including clipping, tone reservation (TR), tone injection (TI), coding, PTS, and SLM. These PAPR reduction techniques are compared according to corresponding criteria. In chapter 4 of the thesis, some modi-

fied SLM schemes with effective PAPR reduction performance or low computational complexity is reviewed. The TPPW-SLM, the PPPW-SLM, and a new low complex SLM scheme are proposed in chapter 5. In this chapter, the TPPW-SLM by employing the IFFT properties is first presented. This chapter also gives the PPPW-SLM, which combines a low complex SLM scheme with a simplified phase optimization process. Lastly, a low complex SLM scheme that combines QAM signals construction with circular convolution is proposed. In Chapter 6, general comparisons among these three proposed low complex PAPR reduction schemes in terms of computational complexity reduction and PAPR reduction performance are studied. The conclusion and suggested future work are discussed in chapter 7.

2 THE BASIS AND STRUCTURE OF OFDM SYSTEMS

OFDM is a special form of multicarrier modulation (MCM), which converts high-speed data streams into a number of low-speed data streams that are transmitted on subcarriers that are mutually orthogonal. Since OFDM makes the symbol duration larger than the spread delay of the communication channel, ISI caused by multipath propagation is negligible (and even can be completely eliminated by adding guard intervals). Moreover, since the subcarriers of an OFDM signal are mutually orthogonal in the time domain, these signals have significant overlap in the frequency domain. Therefore, OFDM has the highest spectral efficiency among all the variants of MCM. Hence, OFDM is currently applied in many wireline and wireless applications. For example [16], the physical layer (PHY) of the IEEE802.16d uses 256 subcarriers OFDM modulation, with 1.75MHz to 20MHz bandwidth; the PHY of the orthogonal frequency division multiple access (OFDMA) uses 2048 subcarriers, with 1.25MHz to 28MHz bandwidth. The IEEE802.16e adds scalable OFDMA, which allows systems to change the number of subcarriers.

This chapter introduces some important fundamentals of OFDM systems, including modulation and demodulation, IFFT/FFT, and some key techniques in OFDM systems. Moreover, the structure of an OFDM system is also presented in this section.

2.1 Background knowledge of the OFDM system

2.1.1 OFDM vs FDM

OFDM is a bandwidth-efficient version of MCM. The main difference between frequency division multiplexing (FDM) and OFDM is that in OFDM, the use of orthogonal subcarriers allows spectral overlapping among the subcarriers without intercarrier interference (ICI), thus increasing the spectral efficiency. Whereas, in an FDM sys-

tem, in order to avoid ICI, guard bands are introduced between adjacent modulated subcarriers. Adding these guard bands decreases the spectral efficiency of the system. Fig. 2.1 illustrates the difference between FDM, which can be considered as the conventional non-overlapping MCM technique, and OFDM, which is the overlapping MCM technique.

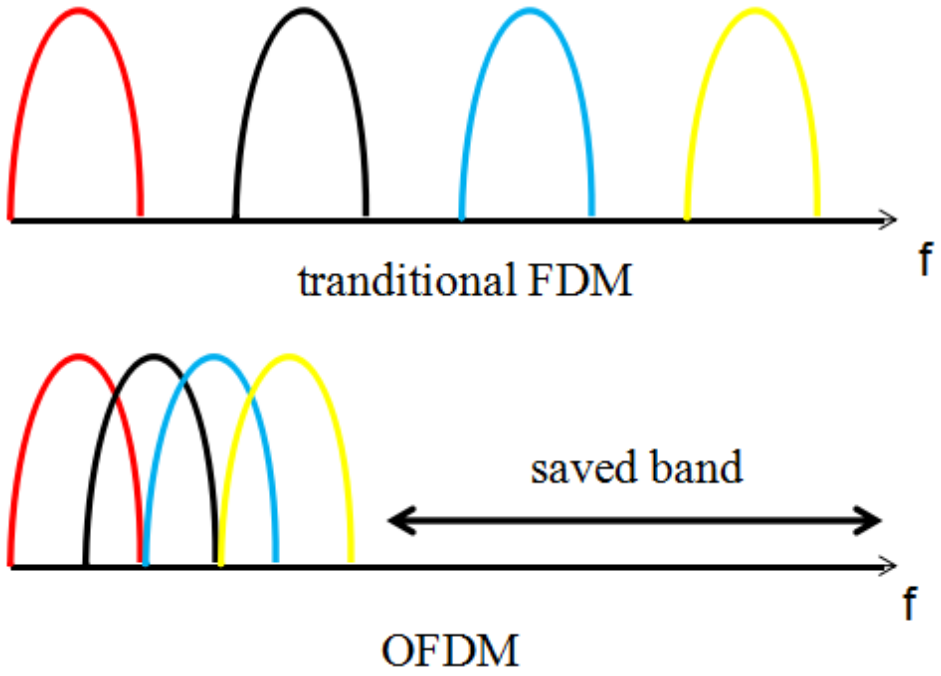

Fig. 2.1: Comparison on bandwidth efficiency for FDM and OFDM.

Compared with single-carrier (SC) modulation, OFDM have some advantages. OFDM is more robust against narrow-band interference, since this type of interference will only affect a small percentage of the subcarriers, while the other subcarriers will not be affected by the interference. Also, OFDM has more immunity to impulsive noise (impulsive noise consists of relatively short duration on/off noise pulses, caused by a variety of sources, such as switching noise, adverse channel environments in a communication system, dropouts or surface degradation of audio recordings, clicks from computer keyboards. etc) [17], since each subcarrier has a lower information rate, the data symbol intervals are longer. Moreover, since the subcarriers of an

OFDM system are mutually orthogonal over the symbol interval, the demodulation of OFDM signals can be implemented much easier.

2.1.2 The fundamental principles of OFDM

The block diagram of an analog OFDM is shown in Fig. 2.2. In an OFDM system with N subcarriers, suppose that the complex symbol X_n is the signal point from the quadrature phase shift keying (QPSK) or quadrature amplitude modulation (QAM) signal constellation that is modulated on the nth subcarrier. The transmitted OFDM signal can be expressed as follows [14]:

$$x(t) = \sum_{n=0}^{N-1} X_n \exp(j2\pi f_n t), \quad 0 \le t \le T, \tag{1}$$

where $f_n = f_0 + n/T$ and $T = NT_s$ is the OFDM symbol interval and T_s is the data symbol period.

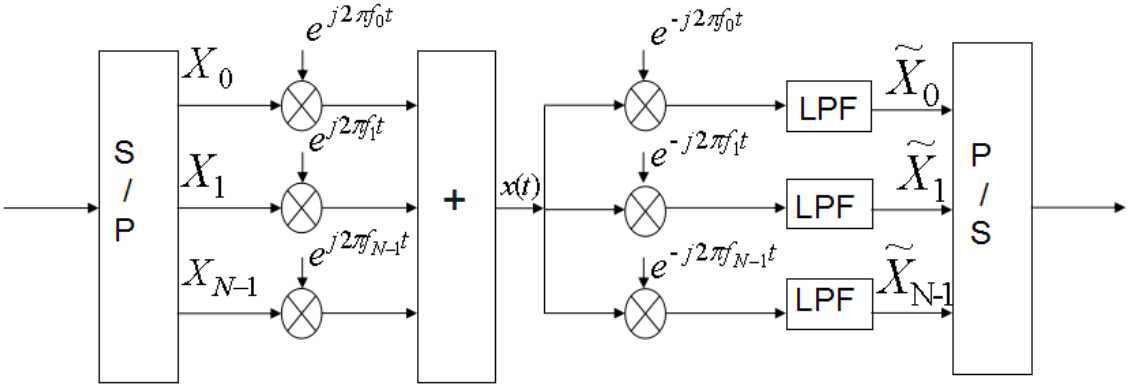

Fig. 2.2: Basic block diagram of OFDM.

In practice, the subcarriers may have different phases and amplitudes because of different complex symbols; however, the subcarriers are mutually orthogonal over the

symbol interval T if the subcarrier spacing is a multiple of $1/T$, as

$$\frac{1}{T}\int_0^T \exp(j2\pi f_n t)\exp(-j2\pi f_m t)dt = \begin{cases} 1, & m = n, \\ 0, & m \neq n, \end{cases} \tag{2}$$

where $|f_n - f_m| = k/T$, $k = 0, \ldots, N-1$.

In order to recover the original data symbols, at the receiving terminal, the received signal $s(t)$ is fed to a bank of N correlators whose outputs are sampled at the end of each symbol interval $t = T$, as illustrated in Fig. 2.2. Since the subcarriers are orthogonal, the correlator outputs can be simply obtained as follows:

$$\begin{aligned} \tilde{X}_k &= \frac{1}{T}\int_0^T x(t)\exp(-j2\pi f_k t)dt, \\ &= \frac{1}{T}\int_0^T \Big[\sum_{n=0}^{N-1} X_n \exp(j2\pi f_n t)\Big]\exp(-j2\pi f_k t)dt, \\ &= \sum_{n=0}^{N-1} X_n \Big[\frac{1}{T}\int_0^T \exp(j2\pi f_n t)\exp(-j2\pi f_k t)dt\Big], \\ &= X_k, \end{aligned} \tag{3}$$

for $k = 0, \ldots, N-1$.

Note that the subcarriers of an OFDM signal can be mutually orthogonal over the symbol interval T, if the frequency separation of the adjacent subcarriers is $1/T$. Based on this condition, the spectral overlapping among the orthogonal subcarriers of an OFDM signal can be easily explained by rectangular windowing of the signal in the time domain, [14]. Since the Fourier transform of a rectangular pulse with duration T, denoted by $\Pi(t/T)$, is a sinc function with zero crossings every $1/T$ Hz, the spectrum of each subcarrier due to windowing becomes a sinc shape with zero crossings (spectral nulls) every $1/T$ Hz. This can be confirmed by taking the Fourier transform of the product of the rectangular pulse $\Pi(t/T)$ and the transmitted signal

$x(t)$ in (1), which is the superposition of all the individual subcarriers, as

$$\begin{aligned}\mathscr{F}[\Pi(t/T)x(t)] &= \mathscr{F}[\Pi(t/T)] \star \mathscr{F}\Big[\sum_{n=0}^{N-1} X_n \exp(j2\pi f_n t)\Big], \\ &= T\text{sinc}(fT) \star \Big[\sum_{n=0}^{N-1} X_n \delta(f - f_n)\Big], \\ &= T\sum_{n=0}^{N-1} X_n \text{sinc}[(f - f_n)T],\end{aligned}$$

where $\star$ denotes the convolution.

Hence, the spectra of different subcarriers overlap, but each subcarrier is in the spectral nulls of all other subcarriers. In other words, the peak point of each subcarrier in the frequency domain corresponds with the zero crossings of the other subcarriers. As a result, the receiver can easily recover the data symbols by sampling the received signal in the frequency domain at the peak points of the sinc functions, where the interference from all other subcarriers, known as intercarrier interference (ICI), is zero.

2.1.3 IFFT/FFT in OFDM systems

Analog implementation of an OFDM system would require multiple local oscillators (LO) that could operate with little drift, in order to retain orthogonality among its subcarriers. This is not a practical solution. The success of OFDM is based on its digital implementation which can be easily implemented using the fast Fourier transform (FFT), which is simply the efficient computational tool for the discrete Fourier transform (DFT).

The OFDM signal in (1) can be synthesized by the inverse discrete Fourier transform (IDFT). Sampling the signal $x(t)$ with sample rate T/N yields the following samples

$$x_k = x(kT/N) = \sum_{n=0}^{N-1} X_n \text{exp}(j\frac{2\pi}{N}nk), \qquad k = 0, \ldots, N-1. \tag{4}$$

The equation (4) is essentially the IDFT of the original symbols X_n. Hence, at the receiving terminal, in order to recover the original symbols X_n, the receiver performs the DFT on the received samples x_k, as

$$X_n = \sum_{k=0}^{N-1} x_k \exp(-j\frac{2\pi}{N}nk), \qquad n = 0, \ldots, N-1. \tag{5}$$

According to the above equations, the IDFT and DFT can simplify the implementation of the modulation and demodulation processes in OFDM systems. The symbols d_n are transformed into the time domain samples s_k by an N-point IDFT. Then using a parallel to serial converter, these N samples can be transmitted one after the other.

In practice, IDFT/DFT can be replaced by IFFT/FFT. The IFFT can decrease the computational complexity. According to the DIF decomposition algorithm that is mentioned in Ref. [18], a N-point IDFT needs N^2 complex multiplications while the Radix-2 IFFT needs only $(N/2)\log_2 N$ complex multiplications, making it a more efficient approach due to decreased computational complexity. Also, the Radix-4 IFFT can be used when N is large enough. An IFFT-based OFDM system is shown in Fig. 2.3.

2.2 The architecture of OFDM systems

2.2.1 Guard interval and cyclic prefix

A main reason why OFDM has been widely applied is that OFDM can resist the spread delay caused by multipath propagation. OFDM systems use serial to parallel (S/P) converters to convert high-speed serial data streams into N parallel low-speed data streams on subchannels. By doing so, the period of the OFDM symbol is expanded, which becomes N times of the input symbol period. Therefore, the corresponding ratio of the spread delay to the symbol period decreases N times. In order to eliminate ISI, a guard interval (GI) can be inserted into OFDM symbols,

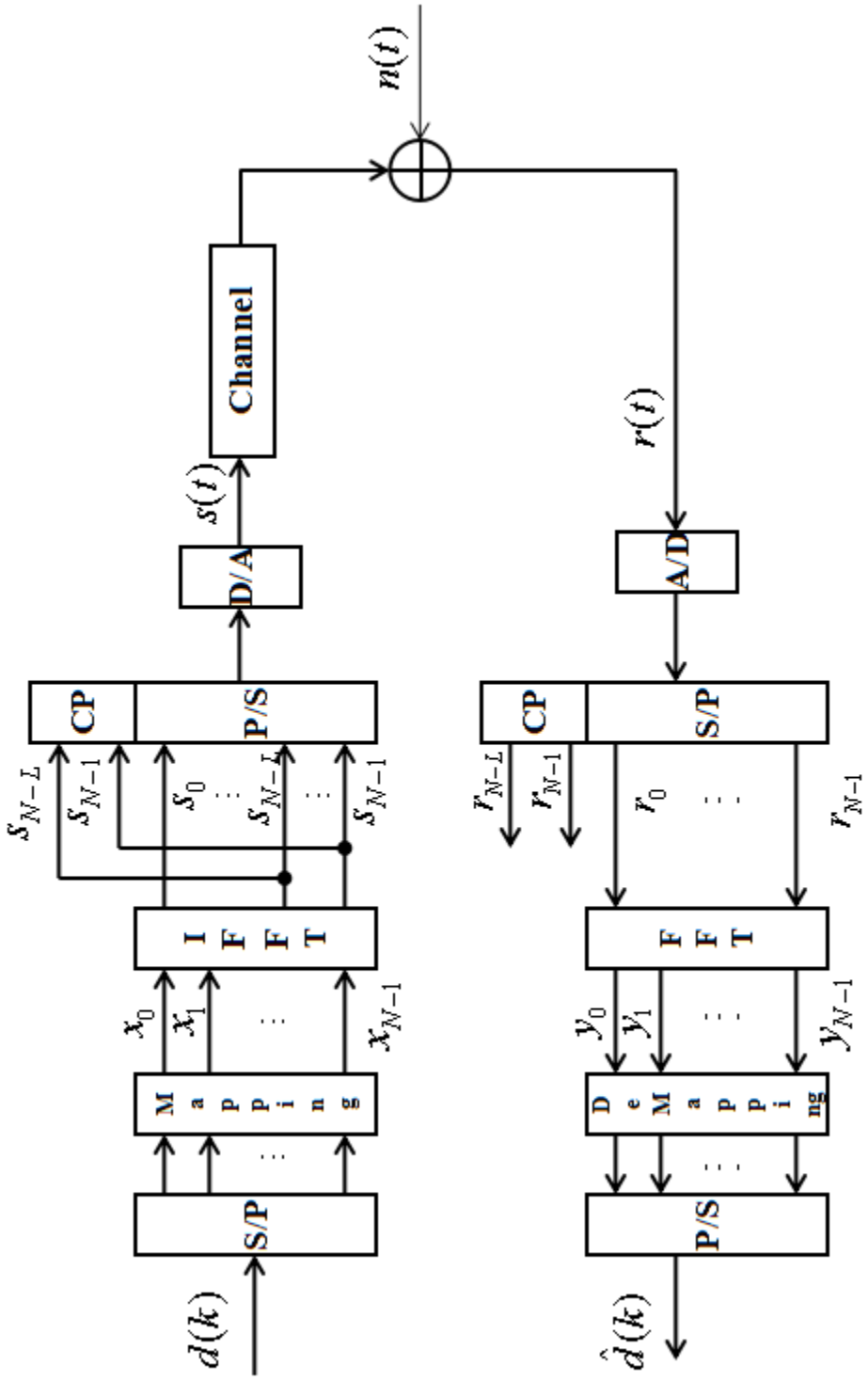

Fig. 2.3: An IFFT-based OFDM system.

and the duration of GI, denoted by T_g, should be longer than the maximum time delay spread. However, if the GI consists of zero samples, there will be interference among sub-channels due to the effect of multipath propagation, which impairs the orthogonality among subcarriers. Hence, in order to eliminate ICI, the CP is added during the GI. The CP is a set of samples that is copied from the data in the last T_g duration of each OFDM symbol. In this way, if the time spread delay is shorter than T_g, signals will not suffer ICI during the demodulation process.

2.2.2 The selection of parameters in OFDM systems

The selection of parameters in OFDM systems is a trade-off. In general cases, three parameters need to be selected: bandwidth, bit rate, and the length of GI. The length of GI should be 2-4 times the root-mean-squared (RMS) delay spread in a mobile communication system (800 ns in most cases).

In order to decrease the loss in signal-to-noise ratio (SNR) caused by inserting GI, the symbol period of OFDM should be much longer than that of GI; however, longer symbol periods will increase the complexity of the system, which makes the OFDM system more sensitive to the carrier frequency offset. Hence, the symbol period is usually five times that of GI, which controls the loss of SNR within 1dB.

Finally, after the selection of symbol periods and GI, the number of sub-carriers can be obtained by dividing the bandwidth according to the interval among subcarriers. The interval of subcarriers is determined by the effects of frequency offset and phase stability. The interval of subcarriers needs to overcome the effects caused by the doppler frequency shift. Furthermore, the bit rate of each subchannel is determined by the type of modulation (such as QAM or PSK), and coding efficiency.

2.2.3 The OFDM transceiver

OFDM divides high-speed data streams into low-speed data streams in order to increase the duration of the symbol period on each subcarrier, which dramatically decrease the ISI caused by time dispersive channels. In the conventional FDM, the data is transmitted on several uncorrelated sub-channels. The sub-channels or subcarriers do not overlap in the frequency domain and there are guard bands between adjacent subcarriers. However, in OFDM, because of the orthogonality among subcarriers, spectral overlapping is possible. This way, for a given bandwidth, OFDM uses the spectrum very efficiently. Fig. 2.4 is the block diagram of a typical OFDM transceiver.

At the transmitter, the coding process (convolution coding in general cases) is firstly implemented to decrease the BER. Then, after interleaving, constellation mapping, and pilot insertion, the high-speed symbols streams are divided into low-speed streams by a serial to parallel converter. After IFFT operations, the parallel symbols streams are transformed into serial symbols, and CP are inserted into the original symbols. Finally, the symbols streams are upconverted and transmitted.

At the receiver, after receiving the RF signal and downcoverting, the analog signals are converted to digital signals by an analog to digital convertor (ADC). After timing and synchronization, the CPs are removed from the OFDM signals. Then, the parallel symbols are fed to the FFT block to transform the received samples in from the time domain to the frequency domain. The constellation demapping is implemented to obtain the coded data stream. Lastly, after decoding, the original data stream is recovered.

2.3 Key techniques in OFDM systems

There are a number of key techniques in OFDM systems, including:

2.3.1 Channel estimation

There are two different types of demodulation in wireless communication systems: coherent demodulation and differential demodulation. Coherent demodulation has lower BER and higher spectral efficiency compared with differential demodulation; however, for coherent demodulation, channel estimation is needed at the receiver side. To design channel estimators, two main issues need to be solved. The first issue is how to design pilots, since pilots need to be transmitted periodically in order to track changes of channels because the wireless channel is a fading channel in most cases. The second issue is how to design channel estimators with high accuracy and low complexity.

2.3.2 Peak to average power ratio reduction

A very high PAPR in OFDM systems requires high power amplifiers (HPA) to have a large linear region, which decreases the power efficiency. Moreover, the receivers also need to have amplifiers and A/D converters that have a large linear region. Therefore, a high PAPR decreases an OFDM system's performance and efficiency. To solve this problem, many researchers have proposed different PAPR reduction schemes, such as companding and clipping. This thesis is mainly concentrated on the issue of PAPR reduction.

2.3.3 Synchronization in the time domain and the frequency domain

The frequency offset in signal transmission may break the orthogonality among sub-carriers, which could lead to ICI. Therefore, synchronization is very important in OFDM systems.

2.3.4 Channel coding and interleaving

To improve the performance of digital communication systems, channel coding is one of the most useful techniques. Channel coding can decrease random errors in fading channels and interleaving can decrease the burst errors in fading channels. Moreover, combining interleaving and coding can further improve the performance of systems.

2.3.5 Equalization

In the channels with extremely bad conditions, the CP must be very long to decrease BER, which dramatically decreases the power efficiency, especially for the systems with a small number of subcarriers. In such cases, equalizers can be considered, which decrease the length of the CP and improve the band efficiency; however, the corresponding complexity will increase.

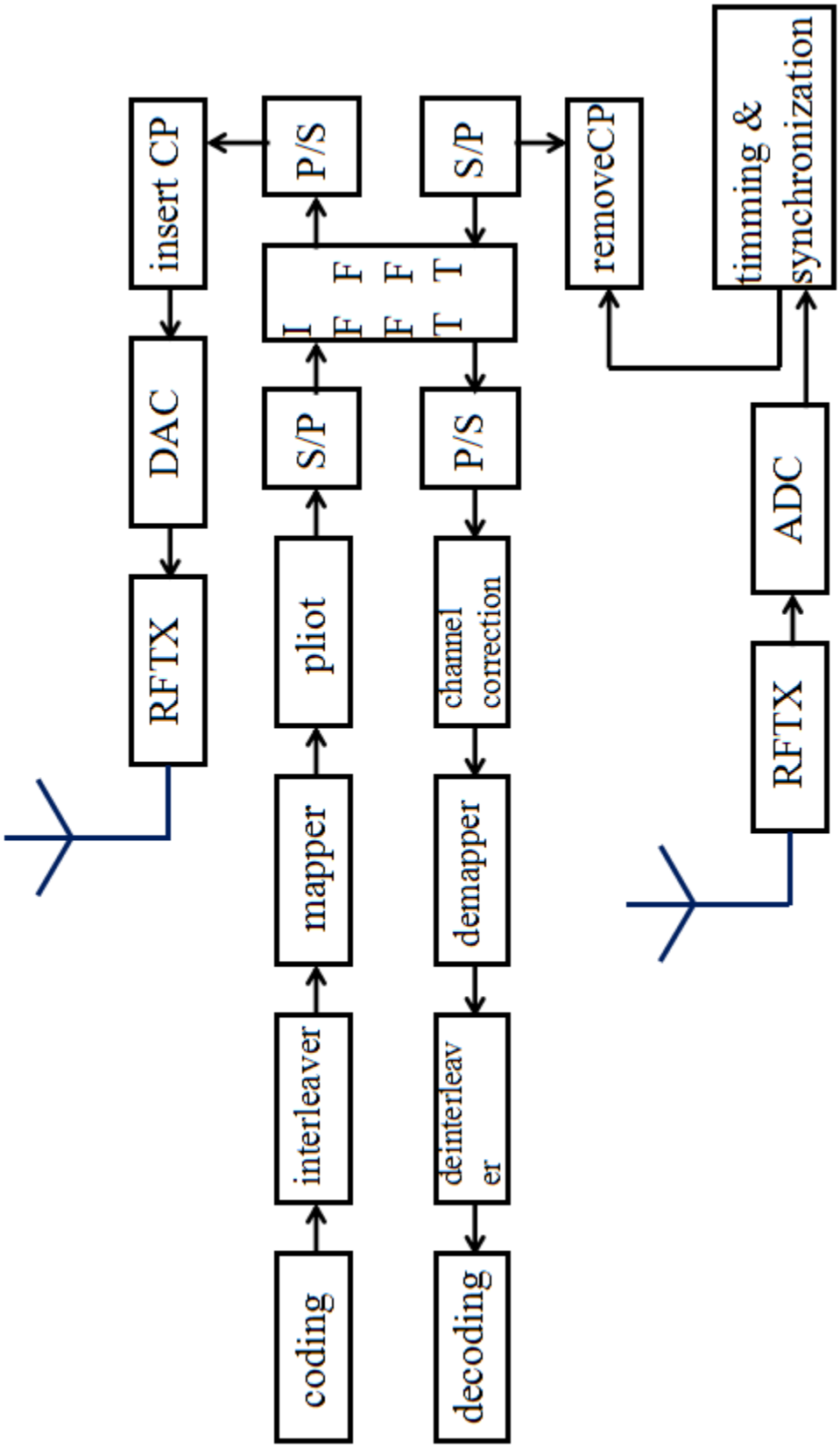

Fig. 2.4: A typical OFDM transceiver.

3 PAPR REDUCTION TECHNIQUES IN OFDM

3.1 Classification of PAPR reduction schemes

It is known that OFDM is robust to the frequency selective fading channels [19]. However, one of the major problems with multicarrier modulation (such as OFDM) is the relatively high peak-to-average- power ratio (PAPR) that is inherent in the transmitted signal. OFDM signals with high PAPR when transmitted through a nonlinear device, such as a high power amplifier (HPA) or a digital-to-analog convertor (DAC) can suffer in-band distortion and out-of-band emission (spectral regrowth). The first effect degrades the BER performance of the system while the latter effect causes interference to other users and thus decreases the cellular capacity of the system, [20]. To avoid such undesirable nonlinear effects, in order to transmit signals with high PAPR without any nonlinear distortions, the radio frequency power amplifier must operate in a wider dynamic linear range which leads to a lower power efficiency [21], which is a significant burden, especially in mobile terminals. Also, the design for A/D and D/A converters is more challenging due to the high PAPR [22].

Various PAPR reduction schemes have been proposed in the literature. Most of these schemes may be classified broadly in the following categories:

- Multiplicative or additive
- Deterministic or probabilistic

In the PAPR schemes that are classified as multiplicative or additive [23] PAPR reduction is carried out in the OFDM modulator. The following two PAPR schemes are considered multiplicative since the input symbols are multiplied by phase rotation factors in the frequency domain:

- Selected mapping (SLM) [24]
- Partial transmit sequence (PTS) [25]

In contrast, the following three schemes are classified as additive since PAPR is reduced by adding some peak reduction vectors to the original input symbols:

- Tone Reservation (TD) [26]
- Clipping [27]
- Peak cancelling [28]

On the other hand, PAPR reduction schemes can be categorized as deterministic or probabilistic [15]. Deterministic schemes are schemes that strictly limit the PAPR of the OFDM signals below a given threshold, such as peak canceling, clipping, and companding schemes. Probabilistic schemes statistically change the distribution of OFDM signals to decrease the probability of the occurrence of peak signals. The SLM, PTS, and interleaving schemes are classified as probabilistic schemes. The SLM and PTS schemes generate a number of candidate signals and take the signal with the minimum PAPR for transmission, and the interleaving schemes [22] decrease the PAPR by scrambling the sequences using different interleavers.

Moreover, the single carrier frequency division multiple access (SC-FDMA) is also an alternative technique to alleviate the high PAPR issue [29]-[30] in OFDM systems. The SC-FDMA is adopted in LTE networks for up-link transmission. When systems are using SC-FDMA, the PAPR is lower than that of OFDM because SC-FDMA transmits symbols in serial format, while OFDM uses parallel transmission. However, in the thesis, the details about SC-FDMA are not discussed.

In this section, different PAPR reduction schemes are compared according to various criteria, including PAPR reduction capabilities, average power increase, BER degradation, data rate loss, computational complexity, and out-of-band radiation [15]. Many researchers have summarized and analyzed the existing PAPR reduction schemes (Ref. [15],[31],[22],[32],[23]). For example, in Ref. [15], Dae-Woon Lim and other two

researchers compared differen PAPR reduction schemes briefly and reviewed some novel low-complex PAPR reduction schemes.

Although numerous schemes have been presented, no specific PAPR reduction schemes can be considered as the best one because all of them have pros and cons. The aim of this chapter is to make a comparison among different conventional PAPR reduction schemes.

3.2 Basis of PAPR in OFDM System

3.2.1 The definition of PAPR

The PAPR of of a continuous-time OFDM signal $x(t)$ can be defined as follows:

$$\text{PAPR}(x) = \frac{\max\limits_{0\le t<T} |x(t)|^2}{\sigma^2}, \tag{6}$$

where σ^2 is the average power of $x(t)$. To make the PAPR computation more practical, the transmitted discrete-time OFDM signal $x[n]$ can be obtained from sampling the continuous-time signal $x(t)$ with sampling period $T_1 = T/N$ as follows:

$$x[n] = \frac{1}{\sqrt{N}} \sum_{k=0}^{N-1} X[k] e^{j2\pi kn/N}, \quad n = 0, \ldots, N-1, \tag{7}$$

where $x[n] = x(nT_1)$. This process can be implemented by N-point IFFT operations, [26].

In other words, PAPR is the ratio of the maximum power and the mean power in one symbol. It can be anticipated that in an OFDM system with N subcarriers, in the worst case PAPR increases linearly with the number of subcarriers N, where $\text{PAPR} = 10\log_{10} N$ in dB. For example, for $N = 256$, PAPR = 24 dB, though it is an extreme case. As shown in Fig. 3.1, where $N = 16$, as an example, the maximum power is 16 times of the mean power because all subcarriers are modulated by symbols

that have the same phase.

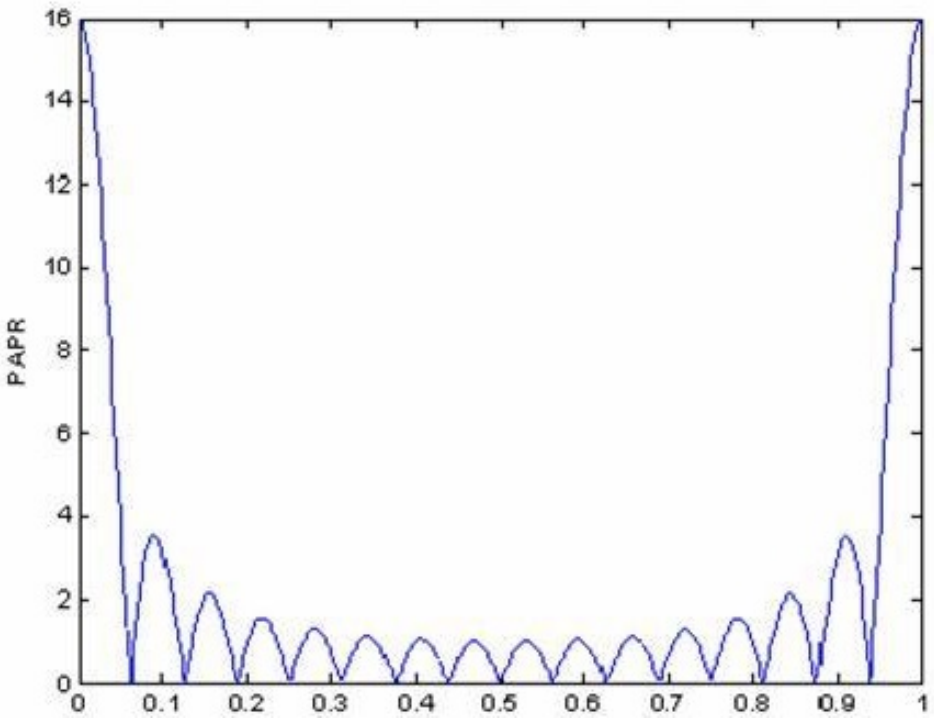

Fig. 3.1: PAPR of an OFDM system with $N = 16$.

3.2.2 The distribution of PAPR

Since the PAPR of an OFDM signal is a random variable, the distribution of the PAPR of dicreate-time baseband OFDM signals is derived here.

If the number of subcarriers is large, by invoking the central limit theorem, it can be shown that both the real and imaginary parts of a discrete-time OFDM signal $x[n]$ are zero-mean Gaussian random variables with variance $\sigma^2/2$, [33]. Because $x[n]$ is a superposition of a large number of modulated signals. Additionally, the power of $x[n]$ has a zero-mean chi-square distribution with two degrees of freedom, and has the complementary cumulative distribution function (CCDF), which is given by

$$F(\alpha) = \Pr\{|x[n]|^2 > \alpha\} = e^{-\alpha}. \tag{8}$$

The CCDF of PAPR for OFDM systems can be approximated as follows:

$$\Pr\{\text{PAPR} > z\} \cong 1 - \exp\Big(- Ne^{-z}\sqrt{\frac{\pi}{3}\ln N}\Big), \tag{9}$$

where all the subcarriers are assumed to be active and have equal power distribution [34]. It should be noted that although the amplitude of $x[n]$ are not statistically independent, the numerical analysis for $N \geq 128$ shows that the approximation of the statistical independence of $|x[n]|$ is quite accurate. Hence, this distribution obtained from (9) is reliable when $N \geq 128$, [15].

3.3 PAPR reduction techniques

A number of approaches have been proposed to deal with the high PAPR issue. In this section, some classical PAPR reduction schemes are introduced. Also, the advantages and disadvantages of these schemes in terms of BER performance, PAPR reduction capability, computational complexity, power increase, spectral efficiency are analyzed. The techniques that are discussed here are: clipping and filtering, companding, coding, PTS, SLM, tone reservation and tone injection.

3.3.1 Clipping and filtering

Since in OFDM signals, the large peak rarely appears, thus clipping and filtering scheme is a very easy and straightforward way to reduce PAPR. This technique is performed in the time domain, where a soft limiter is used to constraint the amplitude of signals under a desirable level. The output signal of a soft limiter can be given by

$$\tilde{x}[n] = \begin{cases} x[n], & |x[n]| < A_t, \\ A_t e^{j\angle(x[n])}, & |x[n]| \geq A_t, \end{cases} \tag{10}$$

where $x[n]$ is the original signal, $\tilde{x}[n]$ is the output after clipping, A_t is the clipping threshold, and $\angle(x[n])$ is the phase of $x[n]$.

Although clipping is an effective way to mitigate PAPR value under a certain threshold, it may cause in-band distortion and out-of-band radiation. Also, the distortion caused by clipping can be considered as another kind of noise, which results in BER degradation.

Filtering is a good way to overcome the above problem in clipping. In filtering method, the clipped time-domain signals are transformed into the frequency-domain by FFT. Then, the out-of-band signals are set to 0. The filtered signals are then transformed into the time-domain by IFFT. Although filtering can reduce out-of-band radiation, it could cause some peak regrowth, so the signals after clipping and filtering could exceed the clipping threshold. To solve these problems, a repeated clipping and filtering may be used, which takes a number of iterations to reach a desirable amplitude level, but the corresponding complexity increases as well [35]-[36].

Some modified schemes have been proposed in [37] and [38], which use the optimized filter H to filter out-of-band noise. Although these schemes achieve better performance, there is a need to solve a convex optimization problem, which significantly increases the computation complexity. Hence, these schemes have difficulties when they are applied in practice. Windowing technique is a similar way to reduce the peak value by adding a window function to the original OFDM signal. Gaussian, Kaiser, and cosine filters are examples of such window functions. However, because the spectrums of the clipped signals are the convolution of the original signals and window functions, the bandwidth of the signals will increase.

The block diagram of clipping and filtering scheme is shown in Fig. 3.2.

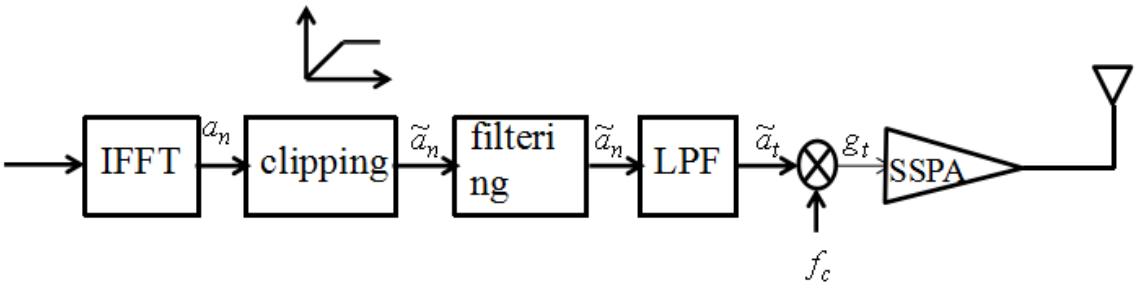

Fig. 3.2: The block diagram of clipping and filtering.

3.3.2 Companding

Some researchers proposed nonlinear processing to reduce high PAPR, through which, the undesirable distortion generated by passing through DAC and HPA can be avoided. Companding is a technique that compresses the signal with high peak and expands the signal with small amplitude. At the receiver side, the inverse action called decompanding is implemented. However, the companding technique makes signal distorted [21]. Therefore, some modified schemes have been proposed to compensate this drawback. Y. Wang, L-H. Wang and J-H. Ge proposed a nonlinear companding with variable companding parameters to achieve good PAPR reduction with lower distortion [39]. Also, it is suggested that the non-symmetric decompanding can improve BER performance for band-limited OFDM systems [40]. Nevertheless, the BER degradation caused by pre-distortion is still not an negligible factor when a companding technique is applied for PAPR reduction.

3.3.3 Coding

One of the well-known techniques for reducing PAPR is block coding, which encodes an input data to a codeword with low PAPR. For instance, the PAPR of OFDM signals with four subcarriers can be reduced by mapping three bits input data to four bits codeword, where parity is added to the last bit in the frequency domain. The

system selects one code with the minimum PAPR for transmission [41].

Coding method can be combined with error correction. Hence, error correction codes are good candidate, which provides PAPR reduction as well as error correction. Golay complementary sequences are good selections for coding, which have zero autocorrelation and non-zero delay shift. Golay complementary codewords ensure that the OFDM signals have at most 3dB PAPR. This property makes Golay codewords attractive in forward error-correction for OFDM systems. Based on this, in Ref. [42], it was presented a specific subset of Golay codes as well as decoding techniques that combined PAPR reduction with forward-error correction capabilities.

There are two drawbacks in coding techniques. First, there is no suitable code for practical OFDM systems with more than 64 subcarriers is known [43]. Second, coding incurs a significant rate loss due to the long code length.

3.3.4 Partial transmit sequence

In PTS [25], the input symbol sequences X are partitioned into V disjoint subblocks of clusters $X^v = [X_0^v, X_1^v, ...X_{N-1}^v]$, where $v = 1, 2, ...V$ (disjoint means for each k, $0 \leq k \leq N-1$, $A_{v,k} = 0$ expect for a single v). The block diagram of PTS is shown in Fig. 3.3.

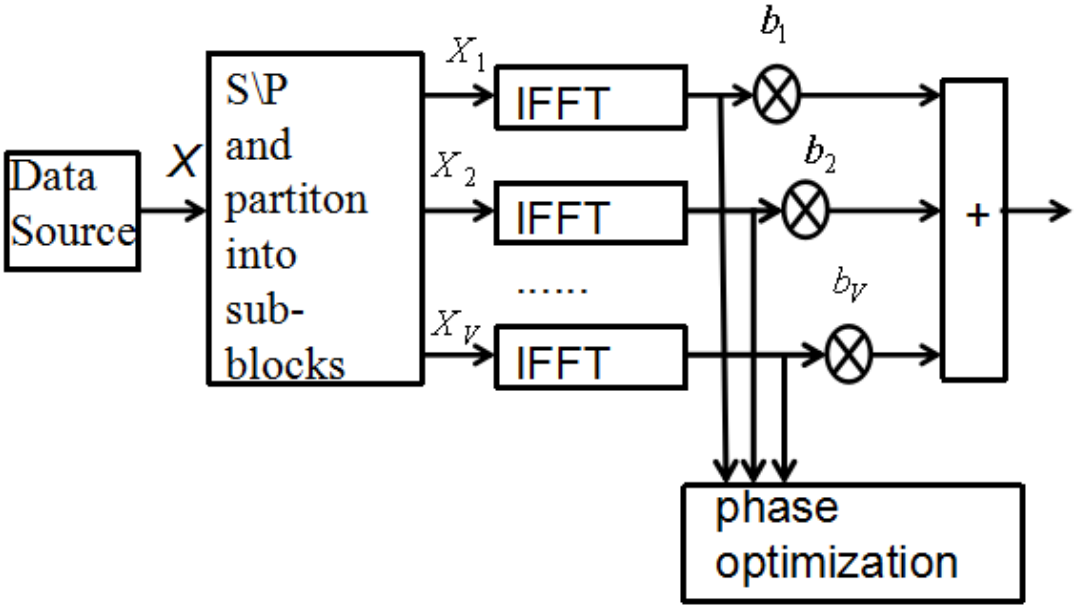

Fig. 3.3: The block diagram of PTS.

The subblocks can be represented as:

$$X = \sum_{v=1}^{V} X_v. \tag{11}$$

After a set of IFFT operations, the time domain sub-vectors $x_v = [x_0^v, x_1^v, ...x_{N-1}^v]$, where $v = 1, 2, ...V$ are multiplied by a set of phase rotation factors b_v^m, where $b_v^m = e^{j\theta_v}$. In general cases, b_v^m is taken from a phase rotation factors alphabet W, which is [1,-1] or [1,-1,i,-i] for simplicity. Then the sub-vectors are added and a PTS OFDM signal is generated, the PTS OFDM signal $x^m = [x_0^m, x_1^m, ...x_{N-1}^m]$ can be expressed as follows:

$$x^m = \sum_{v=1}^{V} b_v^m x_v, \tag{12}$$

where $b^m = [b_1^m, b_2^m, ...b_V^m]$, $1 \leq m \leq M, M = |W|^{V-1}$ are called phase rotation factors. Then, M different candidate PTS OFDM signals are compared, and the system selects

one that has the minimum PAPR for transmission, as

$$\tilde{m} = \arg \min_{1 \leq m \leq M} \text{PAPR}\{x^{(m)}\}. \tag{13}$$

In order to recover the input data, the receivers needs to know the index of $\tilde{m}$.

In general cases, the system needs to do exhaustive search to find the best phase rotation factors combination, for example, if there are 4 subblocks, the system has to find the best phase rotation factors from $2^{(4-1)} = 8$ candidate sequences (if $W = 2$ and the first element of the phase rotation factors is fixed to 1). In other words, the performance and the computational complexity of the PTS scheme is dominated by the number of subblocks and candidate sequences. Hence, the conventional PTS scheme has to suffer high computational complexity in order to get an efficient PAPR reduction performance.

Some modified PTS scheme have been proposed to reduce complexity. For example, in Ref. [44], a low complex PTS scheme called "grouping and recursive phase weighting method" was presented by exploiting the inner-relationship between phase rotation factors. The system saves the same part of phase rotation factors in advance and uses them when a new phase rotation factor is generated.

3.3.5 Selected mapping

SLM is another PAPR reduction scheme based on probability. It is similar to PTS, which uses phase rotation factors to change the distribution of the signal. SLM generates enough number of candidate sequences, and then selects one that has the minimum PAPR for transmission. The difference between SLM and PTS is that in PTS the original data are rotated by phase rotation factors in subgroups after IFFT while in SLM the original data are rotated one by one before IFFT. This subsection presents a brief introduction about the SLM scheme in PAPR reduction for OFDM

system.

The concept of the SLM was firstly presented in Ref. [24]. The conventional SLM scheme is a distortion-less scheme for PAPR reduction [45]. In the SLM scheme, U copies of data, which have equivalent information, are multiplied by U different phase rotation factors. Then the algorithm selects the sequence with minimum PAPR for transmission. The block diagram of the SLM is as follow:

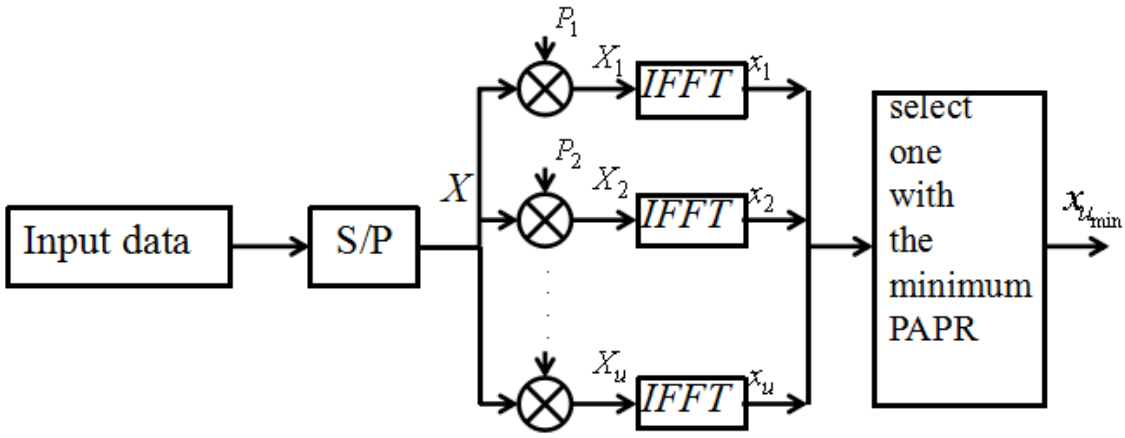

Fig. 3.4: The block diagram of the conventional SLM.

The system generates U signal sequences X, which contain the same information. Then the system multiplies the U signal sequences by U different phase rotation sequences with length N,

$$P^{(u)} = [P_0^{(u)}, P_1^{(u)}, ...P_{N-1}^{(u)}], \quad u = 0, \ldots, U,$$

where $P_i^{(u)} = e^{j\phi_i^{(u)}}$. In general cases, phase rotation factors are taken from $[1, -1, j, -j]$ or $[1, -1]$ and $P^{(0)}$ is a unit vector (all its elements are one). Then the candidate sequences $X^{(u)} = [X_0^{(u)}, X_1^{(u)}, ...X_{N-1}^{(u)}]$ where $X^{(u)} = X_i P_i^{(u)}$ are transformed by IFFT, which is used to create $x^{(u)} = \text{IFFT}[X^{(u)}]$.

After U N-point IFFT operations, the SLM scheme selects the sequence with the lowest PAPR that is denoted by $x_n^{\tilde{u}}$ from U candidate sequences for transmission [45], as

$$\tilde{u} = \arg \min_{0 \leq u \leq U-1} \text{PAPR}\{x_n^{(u)}\}. \tag{14}$$

To recover the data, for simplicity, the receivers generally need to have the table of U different N length phase rotation $P_n^{(u)}$. Hence, just like in PTS, in order to get the index for data recovery, the receiver must know $\tilde{u}$. Thus the transmitter needs to send $\log_2(U)$ bits to pick $\tilde{u}$ from U index sets. These bits are called side information (SI), which decreases the data rate and efficiency. Many researchers have proposed algorithms such as blind or semi-blind data recovery techniques only based on received data or some pre-known data, such as pilot, [20],[46],[47]. In this thesis, it is assumed that the receivers know the table in advance and the transmitter needs to send $\log_2 U$ bits SI to the receiver.

Although both PTS and SLM are distortion-less PAPR reduction schemes, SLM has more advantages than PTS. Previously, people argued that PTS and SLM have comparable PAPR reduction performance but the former scheme has lower computational complexity. However, according to Ref. [45], PTS shows advantages on complexity only when less than a specific number of PTS subblocks are used. If the computational complexity of PTS and SLM are fixed, SLM can outperform PTS in terms of PAPR performance since SLM can produce multiple time-domain signals that are independent, while the alternative signals generated by PTS are interdependent.

Hence, SLM has more advantages than PTS [45]:

1. SLM has lower computational complexity

2. SLM does not need any off-line complexity optimization with respect to the number of sub-blocks V though it is recommended for PTS,

3. SLM has more effective PAPR reduction performance than optimized PTS.

3.3.6 Tone reservation

TR is a distortion-less PAPR reduction technique proposed by Tellado [26]. The term of "Tone" represents the subcarrier because TR is firstly developed for a DSL system and subcarriers are called tones in a DSL system. The TR scheme uses a part of tones which is called peak reduction tone (PRT) to decrease PAPR. In most cases, PRT do not contain any information data and they are adeed to original OFDM signals to generate new signals with lower PAPR. There are two two types of TR scheme: clipping based TR and gradient based TR.

The PAPR reduction performance of TR is based on the PRT set and clipping threshold [48], which is a NP-hard problem. Because the kernel p must be optimized over all possible discrete sets R, thus, it cannot be solved for practical subcarrier numbers. The Ref. [49] and Ref. [48] discussed such problems and proposed near optimal PRT algorithms. However, in this subsection, only the conventional TR scheme is discussed.

Let $X = [X_0, X_1, ..., X_{N-1}]$ be the original input frequency domain symbols, and $C = [C_0, C_1, ...CN-1]$ be the PRT signals in frequency domain. Hence, the time domain OFDM signals after peak reduction can be given as follows:

$$a = x + c = Q(X + C), \tag{15}$$

where Q is the IFFT matrix. In order to avoid signal distortion, the X data symbols and C PRT signals should be disjoint. In other words, if $R = p_1, p_2, ...p_m$ denotes the ordered set of the positions of the reserved tones and $N = [0, 1..., N-1]$ denote the

set of subcarriers. The input frequency domain symbols A can be written as follows:

$$A_k = \begin{cases} C_k, & k \in R, \\ X_k, & k \in R^c, \end{cases} \tag{16}$$

where R^c is the complement set of R.

Because of the linearity of the IFFT. The PAPR in TR scheme is shown as follows:

$$\mathrm{PAPR}(a) = \frac{\max\limits_{0 \le n \le N-1} |a_n|^2}{\frac{1}{N} \sum\limits_{n=0}^{N-1} E[|x_n|^2]}, \tag{17}$$

where $|a_n|^2 = |x_n + c_n|^2$.

Then, in the conventional TR scheme, the PRT signals are generated iteratively. Let $p = [p_0, p_1, ..., p_{N-1}]$ denote the time domain kernel which is defined as follows:

$$p_n = \frac{1}{\sqrt{N}} \sum_{k \in R} P_k e^{j2\pi t \frac{k}{N}}, \tag{18}$$

where P_k is the frequency domain kernel and $P_k = 0$ when $k \in R^c$, where R^c is the complementary set of R. Next, the time domain kernel p are used to compute peak reduction signals c iteratively, [23]. Let v denotes the number of iterations, thus the v_{th} peak reduction signals c^v are

$$c^v = \sum_{i=1}^{L} a_i p_{\tau_i}, \tag{19}$$

where p_{τ_i} is a circular shift of p by τ_i and a_i is a complex scaling factor which is computed according to the threshold and the maximum peak value at the i_{th} iteration. The value of τ_i can be determined according to the equation as follows:

$$\tau_i = \arg \max_{0 \le n \le N-1} |x_n + c_n^{i-1}|. \tag{20}$$

Next, the OFDM signal $a = x + c^m$ in the TR scheme can be generated.

It should be noted that the iteratively generated peak reduction signal sequence does not affect the data symbols because of the shift property of IFFT. By making use of the shift property of IFFT, the value of $Q^{-1}p_{\tau_i}$ and $C^v = Q^{-1}c^v$ is always 0 when they are in R^c, where Q^{-1} is the inverse matrix of Q.

3.3.7 Tone injection and active constellation extension

Although TR schemes achieve efficient PAPR reduction performance, PRT could waste valuable subcarriers, which significantly decrease the data rate. The tone injection (TI) scheme can be used to reduce PAPR without data rate reduction. In the TI scheme, the PRT are overlapped with data tones. The main idea of TI is to increase the constellation size so that each of the point in the original constellation can be mapped into several equivalent points in the new expanded constellation where the extra degrees of freedom can be obtained to reduce PAPR [50]. In other word, the time domain PAPR reduced signals can be generated from the different combinations of the overlapped data signals and peak reduction signals.

Active constellation extension (ACE) [32] is to pre-distort the input symbols before IFFT to decrease the PAPR. In the ACE scheme, only the outer constellation symbols can be predistorted in order to keep the minimum distance of the constellation unchanged. In this way, there is no BER degradation at the receiving side. In the ACE, points in the side of the constellation are moved along the half-line in the outer direction, while points in the corner of the constellation can be moved in larger quadrant area. The advantages of ACE scheme are no data loss and no SI; however, in order to maintain the minimum distance, the ACE may cause peak regrowth, which increases the average power and the amount of iterations.

Actually, TI and ACE schemes are modified versions of TR. Both these two schemes need to change the size of constellation. In other words, adding extra signals

Table 3.1: Comparison among different PAPR reduction schemes.

	PRC	API	BER	DRL	CC	OBR
clipping	Good	N	Y	N	Low	Y
companding	Good	N	Y	N	Mid	Y
coding	Good	N	N	Y	High	N
PTS	Good	N	N	Y	High	N
SLM	Good	N	N	Y	High	N
TR	Good	N	N	Y	High	N
TI	Good	Y	N	N	High	N

with more power into the original constellation of the OFDM signals increases the transmitting power. Furthermore, compared with TR, ACE and TI need to solve a more complicated nonlinear constrained optimization problem, which makes these two schemes unpopular.

There are also some other PAPR reduction schemes besides clipping, coding, and probabilistic techniques, such as interleaving [51], pilot sequences [52], m-sequences [53]. Although these techniques can reduce PAPR, some of them need nonlinear transformation, some of them do not have efficient PAPR reduction performance. Hence, these methods are not popular.

Table 3.1 is a brief comparison among different kind of PAPR reduction schemes with the respect of PAPR reduction capability (PRC), average power increase (API), BER depredation (BER), data rate loss (DRL), computational complexity (CC), and out-of-band radiation (OBR). It should be noted that the comparison of SLM and PTS has been done in former subsection.

4 MODIFIED SLM SCHEMES

SLM is a probabilistic PAPR reduction scheme that can significantly reduce the PAPR of OFDM signals with no distortion and BER performance degradation. On the other hand, one of its drawbacks is its high computational complexity compared with other PAPR reduction techniques. Hence, the problem of modifying the SLM scheme has been investigated by many researchers and some modified SLM have been proposed schemes [21], [54], [55], [20]. In the literature, there have been two types of research on modifying the SLM scheme with the following objectives:

- how to improve the PAPR reduction performance of SLM,
- how to decrease the computational complexity of SLM.

In this section, two modified SLM schemes are reviewed. One of these schemes gives better PAPR performance, and the other one significantly decreases the computational complexity compared with the conventional SLM scheme.

4.1 Bit-based SLM schemes

In order to improve PAPR reduction performance without increasing computational complexity, the randomness among candidate sequences can be increased. This can be achieved by decreasing the correlation among candidate sequences. It is shown in Ref. [56] that a set of U phase sequences with lower variance of correlation (VC) in the SLM scheme gives better PAPR reduction performance. In Ref. [21], the partial bit inverted SLM (PBISLM) using QAM modulated signals was proposed by Hyun-Bae Jeon. Compared with the conventional SLM, which rotates the phases of QAM symbols after constellation mapping, the proposed scheme changes the magnitudes as well as the phases of QAM symbols by applying the binary phase rotation sequences to binary data sequences before mapping to QAM signals. This scheme can achieve

more PAPR reduction than the conventional SLM scheme with a little more cache required, which can be neglected in practice.

Let A be the input symbol sequence of length N after M-QAM modulation. The binary format of A of length $N \log_2 M$ can be expressed as follows:

$$A_B = [A_{0,0}, ..., A_{0,m-1}, ..., A_{N-1,0}, ..., A_{N-1,m-1}], \tag{21}$$

where $m = \log_2 M$, and $A_{k,l} \in \{1, -1\}$ is the lth bit of the kth M-QAM symbol. In PBISLM, the candidate symbol sequences are generated by multiplying some pre-selected bits of each M-QAM symbol $A_k^{(u)}$ by $P_k^{(u)}$ in the binary phase sequence $P^{(u)} = [P_0^{(u)}, P_1^{(u)}, ..., P_{N-1}^{(u)}]$, $0 \leq u \leq U$, $P_k^{(u)} \in \{+1, -1\}$. Let $S = \{0, 1, ..., L-1\}$ be a subset of bit indices $L = \{0, 1, ..., \log_2 M - 1\}$ for M-QAM symbol and S^C be the complement set of S in L. The lth bit $X_{k,l}^{(u)}$ of the kth symbol in the binary form of the uth alternative symbol sequence can be expressed as follows:

$$X_{k,l}^{(u)} = \begin{cases} A_{k,l} P_k^{(u)}, & l \in S, \\ A_{k,l}, & l \in S^C. \end{cases} \tag{22}$$

If $P_k^{(u)} = -1$, the bits of A_k corresponding to S are inverted and thus $A_k^{(u)}$ is mapped to another M-QAM symbol $X_k^{(u)}$. After the IFFT operations of candidate symbol sequences $X^{(u)}$, the OFDM signal sequences $x^{(\tilde{u})} = \text{IFFT}[X^{(\tilde{u})}]$ with the minimum PAPR is selected for transmission.

Since OFDM signals with small number of N do not follow the complex Gaussian distribution, this scheme uses joint cumulates up to the fourth order instead of covariance to determine if two alternative sequences are independent or not.

In order to guarantee that the covariance of average symbol powers of alternative symbol sequences stays as low as possible, 16-QAM and 64-QAM are investigated, and the covariance between two candidate sequences for PBISLM with M-QAM are

generalized. For simplicity, in this subsection, only 16-QAM is applied as an example. More details can be found in Ref. [21].

Fig. 4.1 shows a Gray mapping for 16-QAM constellation. If $S = \{0, 1, 2, 3\}$ and $S^C = \emptyset$ are used, all bits for the kth input symbol are inverted when $P_k^{(u)} = -1$, which is given by Fig. 4.1. Assuming that $E[|A_k|^2]$, the input symbols A_k are classified into three subsets E_1,E_2,and E_3 according to their powers such that $E_1 = \{0000, 1000, 1010, 0010\}$ with symbol power $P_1 = 0.2$,

$$E_2 = \{0100, 0001, 1001, 1100, 1011, 0011, 0110\}$$

with symbol power $P_2 = 1.0$ and $E_3 = \{0101, 1101, 1111, 0111\}$ with symbol power $P_3 = 1.8$. Then the amplitude gain $\Lambda_k^{(u)}$ of the symbol in candidate sequences generated by PBISLM is

$$\Lambda_k^{(u)} = \begin{cases} 1, & A_k \in E_2 \quad \text{or} \quad P_k^{(u)} = 1, \\ \sqrt{P_1/P_3}, & A_k \in E_3 \quad \text{or} \quad P_k^{(u)} = -1, \\ \sqrt{P_3/P_1}, & A_k \in E_1 \quad \text{or} \quad P_k^{(u)} = -1. \end{cases} \tag{23}$$

If the phase rotation factors $P^{(u)}$ are balanced in terms of quantity and are randomly generated from the set {+1,-1}, it can be shown that the covariance of average symbol powers of two candidate sequences is 0, as

$$\begin{aligned} \text{cov}(\bar{P}^{(l)}, \bar{P}^{(m)}) &= \frac{1}{N}\big(E[|A_k|^4 |\Lambda_k^{(l)}|^2 |\Lambda_k^{(m)}|^2] - 1\big), \\ &= \frac{1}{N}\Big\{\frac{1}{2}\big(\frac{1}{4}(P_1)^2\big)\frac{P_3}{P_1} + \frac{1}{2} + \frac{1}{4}(P_3)^2\frac{P_1}{P_3} \\ &\qquad + \frac{1}{2}\big(\frac{1}{4}(P_1)^2 + \frac{1}{2} + \frac{1}{4}(P_3)^3\big) - 1\Big\}, \\ &= 0. \end{aligned} \tag{24}$$

Hence, the PAPR reduction performance of PBISLM should be expected to be better

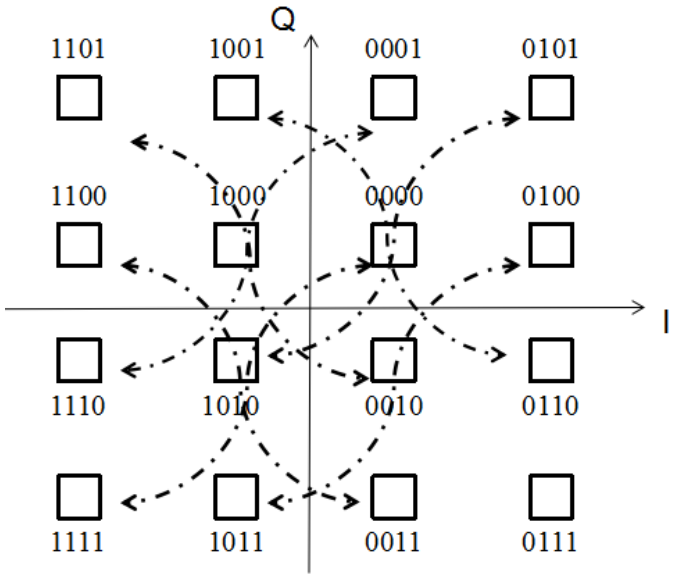

Fig. 4.1: An example of partial bit inversion of Gary mapped 16-QAM constellation for PBISLM.

than that of the conventional SLM scheme because the average symbol powers of candidate sequences in the scheme are uncorrelated with each other.

Fig. 4.2 shows the CCDF performance of PBISLM, the conventional SLM, and BSLM, which is also proposed in Ref. [21], with 16-QAM modulation, 16 candidate sequences and 64 subcarriers.

From Fig. 4.2 [21], it is known that the proposed PBISLM scheme has better PAPR reduction performance than other SLM schemes because of the more randomness among candidate sequences. Although the improvement in the PAPR reduction performance is not so obvious, there is no much computational complexity increase but only by requiring additional memory to save the longer phase rotation factors.

4.2 Modifed Class-III SLM scheme

In [20], a modified version of the SLM scheme using Class-III conversion vectors has been proposed. Although Class-I and Class-II have been presented in Ref. [20], the

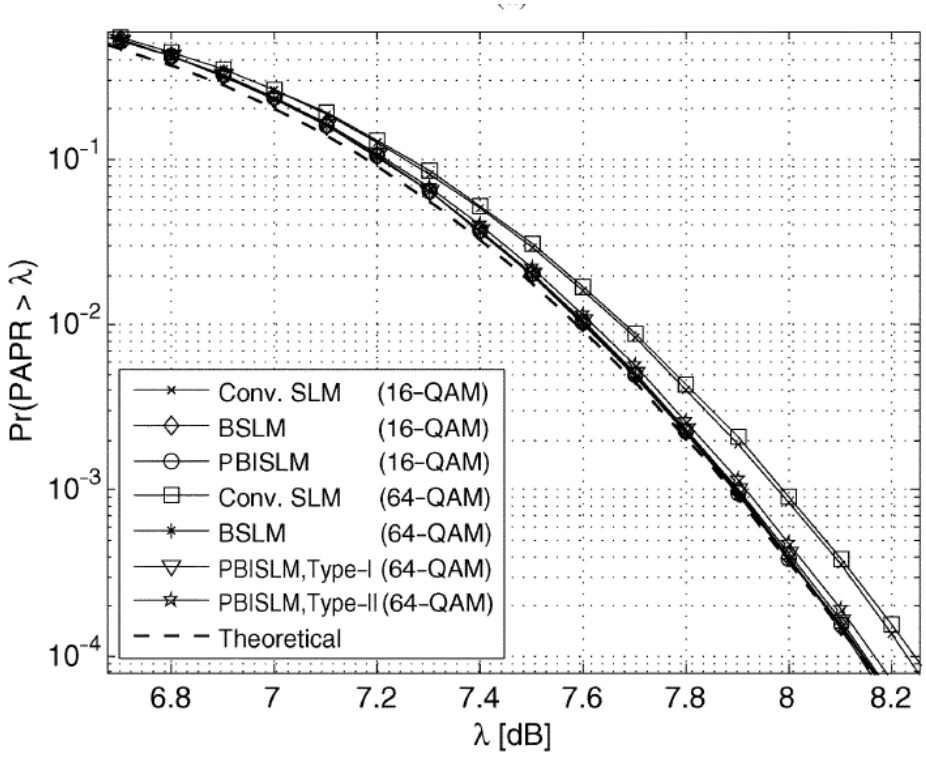

Fig. 4.2: Comparison of PAPR reduction performance of the conventional SLM and proposed schemes for $U = 16$, $N = 64$.

Class-III SLM scheme shows the most efficient PAPR reduction performance than the other two schemes. Thus, this subsection is concentrated on the Class-III SLM scheme and its modified version proposed in [57].

The Class-III SLM scheme requires only one IFFT operation to generate all candidate sequences, which is shown in Fig. 4.3. It is assumed that the input symbols sequences $X = [X_0, X_1, X_2, ..., X_{N-1}]$ have been modulated by M-ary phase shift keying (M-PSK) or M-ary quadrature amplitude modulation (M-QAM), where N is the number of subcarriers or the size of the IFFT. After the IFFT operations, the time-domain OFDM sequence x is transformed by N-point circular convolution with

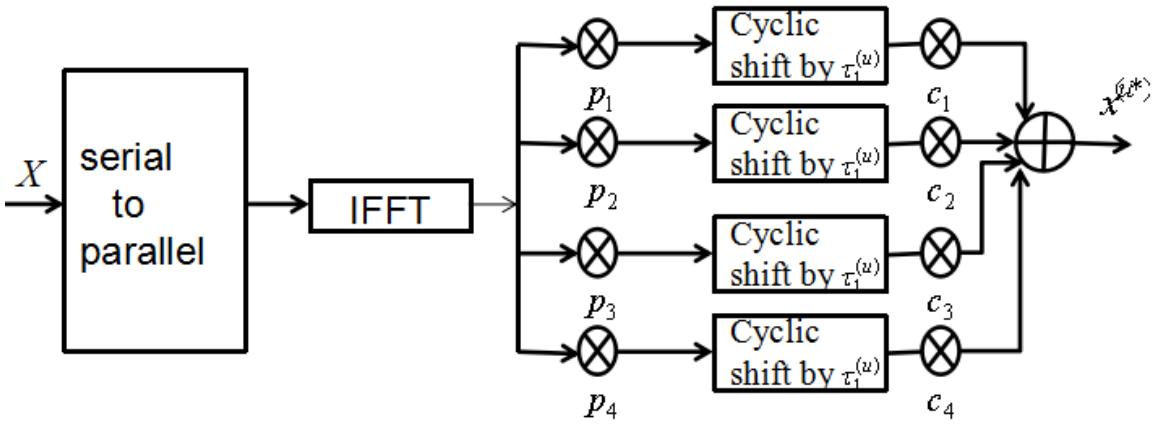

Fig. 4.3: The block diagram of the Class-III SLM scheme.

the following four basis vectors:

$$
\begin{aligned}
p_1 &= [\underbrace{1,0,...,0}_{N/4}\,\underbrace{1,0,...,0}_{N/4}\,\underbrace{1,0,...,0}_{N/4}\,\underbrace{1,0,...,0}_{N/4}],\\
p_2 &= [\underbrace{1,0,...,0}_{N/4}\,\underbrace{j,0,...,0}_{N/4}\,\underbrace{-1,0,...,0}_{N/4}\,\underbrace{-j,0,...,0}_{N/4}],\\
p_3 &= [\underbrace{1,0,...,0}_{N/4}\,\underbrace{-1,0,...,0}_{N/4}\,\underbrace{1,0,...,0}_{N/4}\,\underbrace{-1,0,...,0}_{N/4}],\\
p_4 &= [\underbrace{1,0,...,0}_{N/4}\,\underbrace{-j,0,...,0}_{N/4}\,\underbrace{-1,0,...,0}_{N/4}\,\underbrace{j,0,...,0}_{N/4}].
\end{aligned}
\tag{25}
$$

Then, the ith sequence, for $i = 1, 2, 3, 4$, of four generated sequences is cyclically shifted to the right by $\tau_i^{(u)}$ samples where $\tau_i^{(u)} = 0, \ldots, N/4$ and then rotated by multiplying $c_i^{(u)}$, which is taken from the following set $\{+1, -1, +i, -i\}$, where u is the index of a candidate sequence. Without generality, it is assumed that $\tau_1^{(u)} = 0$, and $c_1^{(u)} = 1$. By adding the four generated sequences, the OFDM candidate sequences $\{x^{(u)}\}$ are generated and the one with the lowest PAPR is transmitted.

Finally, the Class-III conversion vector, denoted by $p^{(u)}$, to generate $x^{(u)}$, can be

written as follows:

$$p^{(u)} = \sum_{i=1}^{4} c_i^{(u)} p_i < \tau_i^{(u)} >, \tag{26}$$

where $p_i < \tau_i^{(u)} >$ denotes the cyclic shifted version of p_i to the right by $\tau_i^{(u)}$ samples. The original Class-III can generate up to N^3 alternative OFDM signal sequences by varying $\tau_i^{(u)}$ and $c_i^{(u)}$, which is a large number in practice. However, in [57], the variance of correlation among different candidate sequences has been analyzed and found out that rotation values are useless when $U > N/8$. Hence, three principles to select the optimal candidate sequences from N^3 alternative OFDM signal sequences in the conventional Class-III SLM shame are proposed, and a selection method of proper rotation values $c_i^{(u)}$ when $U > N/8$ is also given. Based on these principles, the number of candidate sequences is reduced to $N/2$ compared to the conventional Class-III SLM scheme. This way the selection of candidate sequences can be done more effectively. Fig. 4.4 shows the PAPR performance of three PAPR reduction schemes: the modified Class-III SLM, the PAPR reduction scheme previously proposed in [58], and the conventional SLM, [20].

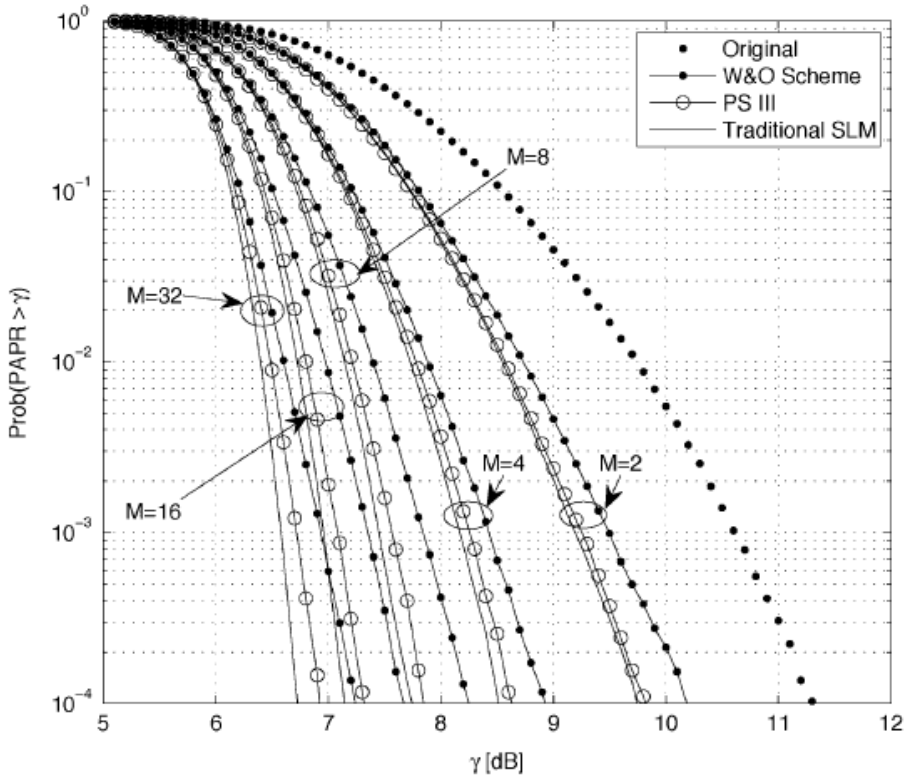

Fig. 4.4: Comparison of the PAPR performance of Class-III and the other schemes.

5 PROPOSED MODIFIED SLM SCHEMES

In this section, three improved low complex SLM schemes with effective PAPR reduction performance are proposed. These three modified SLM schemes are introduced and analyzed. The comparison among three proposed SLM schemes is presented in section. 6.

5.1 The preliminary knowledge of IFFT properties used in the proposed SLM schemes

Some IFFT properties are applied in the first two proposed SLM schemes. Therefore, in this subsection, some IFFT properties used in the proposed SLM schemes are reviewed [54].

A. Circular shift theorem [59]:

A cyclic shifted sequence in the frequency domain can be expressed as the corresponding time domain sequence with phase rotation, which is written as follows:

$$\text{IFFT}\{X^{(k)}\} = \text{IFFT}\{X\}\mathbf{\Theta}W_k, \tag{27}$$

where $X^{(k)}$ represents a shifted version of the OFDM symbol X by k samples (if k is positive, X is cyclically shifted to the right, and if k is negative, X is cyclically shifted to the left), $\mathbf{\Theta}$ denotes component-wise multiplication and

$$W_k = \{1, \exp(j2\pi k/N), ..., \exp(j2\pi k(N-1)/N)\}.$$

Based on (27), the following important equation can be easily obtained as follows:

$$\text{IFFT}\{X\} = \text{IFFT}\{X^{(k)}\}\mathbf{\Theta}W_{(-k)}. \tag{28}$$

B. Up-sampling theorem [60]:

If a sequence with N elements in the frequency domain has the following form:

$$X_m = [X_0, \underbrace{0, ..., 0}_{m}, X_m, \underbrace{0, ..., 0}_{m}, X_{N-m}, \underbrace{0, ..., 0}_{m}] \tag{29}$$

and its corresponding time-domain sequence can be obtained as follows:

$$\begin{aligned} x_{(m)} &= \frac{1}{m}[\text{IFFT}\{X'_m\}, \text{IFFT}\{X'_m\}, \cdots, \text{IFFT}\{X'_m\}] \\ &= \frac{1}{m}[\underbrace{x'_m, x'_m, ...x'_m}_{m}] \end{aligned} \tag{30}$$

where $X'_m = [X_0, X_m, ..., X_{N-m}]$, $x'_m = \text{IFFT}\{X'_m\}$ and m is a power of two.

C. Conjugation theorem [59]:

Assuming that

$$\text{IFFT}\{X\} = [x_0, x_1, ..., x_{N-1}], \tag{31}$$

the time domain sequence corresponding to the complex conjugate of the frequency-domain sequence can be obtained from the symmetry property of the IFFT, as follows:

$$\text{IFFT}\{X^*\} = [x_0^*, x_{N-1}^*, ..., x_1^*]. \tag{32}$$

5.2 A new low complex time domain partial phase weighting SLM

In this subsection, a new low complex SLM scheme called time-domain partial phase weighting SLM (TPPW-SLM) is proposed. In the proposed scheme, some of the

OFDM symbols in the time domain are rotated after IFFT operations, and then the rotated symbols are combined with the rest of symbols by using IFFT properties, which greatly decreases the number of IFFT units. The proposed SLM scheme generates different candidate sequences by employing the IFFT properties and circular convolution in the time domain. Also, the proposed SLM scheme needs to transmit side information as the conventional SLM scheme does.

5.2.1 The main idea of the proposed SLM scheme

In the proposed SLM scheme, first the input symbol X with N subcarriers is partitioned into D disjoint subblocks by an interleaving method, where D is a power of two. In this way, the input data block can be written as follows:

$$X = \sum_{d=1}^{D} X_d. \tag{33}$$

All the subblocks can be given by

$$\begin{aligned}
&X_1 = [X_0, 0, ...0, X_D, 0, ...0, X_{N-D}, 0, ...0], \\
&X_2 = [0, X_1, 0, ...0, X_{D+1}, 0, ...0, ...X_{N-D+1}, 0, ...0], \\
&X_3 = [0, 0, X_2, 0, ...0, X_{D+2}, 0, ...0, ...X_{N-D+2}, 0...0], \\
&..... \\
&X_D = [0, ...0, X_{D-1}, 0, ...0, X_{2D-1}, ...0, ...X_{N-1}].,
\end{aligned} \tag{34}$$

For these subblock sequences, the corresponding time-domain sequences can be obtained based on the "*circular shift theorem*" and "*up-sampling theorem*". To apply the "*up-sampling theorem*" to transform X_d into the time domain, first the left-cyclic shifted of these sub-block sequences are required. The cyclic-shifted sub-block se-

quences are written as follows:

$$\begin{aligned}
&X_1 = [X_0, 0, ...0, X_D, 0, ...0, X_{N-D}, 0, ...0] \\
&X_2^1 = [X_1, 0, ...0, X_{D+1}, 0, ...0, ...X_{N-D+1}, 0, ...0], \\
&X_3^2 = [X_2, 0, ...0, X_{D+2}, 0, ...0, ...X_{N-D+2}, 0...0], \\
&..... \\
&X_D^{D-1} = [X_{D-1}, 0, ...0, X_{2D-1}, 0, ...0, ...X_{N-1}, 0...0],
\end{aligned} \tag{35}$$

where X_d^{d-1}, for $d = 1, 2, 3...D$, denotes that $d-1$ elements of the d^{th} sub-block sequence X_d are cyclically shifted to the left.

After the cyclic shifting operation, by using the "*up-sampling theorem*", the time-domain sequences of the corresponding sub-blocks are obtained as follows:

$$\begin{aligned}
x_1^{(0)} &= \frac{1}{D}[\text{IFFT}\{X_1^{(0)'}\}, ..., \text{IFFT}\{X_1^{(0)'}\}] \\
&= \frac{1}{D}[\underbrace{x_1^{(0)'}, ..., x_1^{(0)'}}_{m}] \\
x_2^{(1)} &= \frac{1}{D}[\text{IFFT}\{X_2^{(1)'}\}, ..., \text{IFFT}\{X_2^{(1)'}\}] \\
&= \frac{1}{D}[\underbrace{x_2^{(1)'}, ..., x_2^{(1)'}}_{m}] \\
&..... \\
x_D^{(D-1)} &= \frac{1}{D}[\text{IFFT}\{X_D^{(D-1)'}\}, ..., \text{IFFT}\{X_D^{(D-1)'}\}] \\
&= \frac{1}{D}[\underbrace{x_D^{(D-1)'}, ..., x_D^{(D-1)'}}_{m}]
\end{aligned} \tag{36}$$

where

$$X_d^{(d-1)'} = [X_d, X_{D+d-1}, ..., X_{N-D+d-1}],$$

and $x^{(d-1)} = \text{IFFT}\{X_d^{(d-1)'}\}$, for $d = 1, 2, ..., D$.

In order to perform partial phase weighting in the time domain, the input symbols

in the first sub-block symbols $x_1^{(0)}$ are transformed by a circular convolution (denoted by $\otimes$) by N/D points with the following four different basis vectors:

$$\begin{aligned}
p_1 &= [\underbrace{1,0,...,0}_{N/4D}\underbrace{1,0,...,0}_{N/4D}\underbrace{1,0,...,0}_{N/4D}\underbrace{1,0,...,0}_{N/4D}],\\
p_2 &= [\underbrace{1,0,...,0}_{N/4D}\underbrace{j,0,...,0}_{N/4D}\underbrace{-1,0,...,0}_{N/4D}\underbrace{-j,0,...,0}_{N/4D}],\\
p_3 &= [\underbrace{1,0,...,0}_{N/4D}\underbrace{-1,0,...,0}_{N/4D}\underbrace{1,0,...,0}_{N/4D}\underbrace{-1,0,...,0}_{N/4D}],\\
p_4 &= [\underbrace{1,0,...,0}_{N/4D}\underbrace{-j,0,...,0}_{N/4D}\underbrace{-1,0,...,0}_{N/4D}\underbrace{j,0,...,0}_{N/4D}].
\end{aligned} \tag{37}$$

After convolution, the k^{th}, $k = 1, 2, 3, 4$ convoluted sequence is cyclic-right shifted by $\tau_k^{(m)}$, where m is the index of optimal shift values and $\tau_k^{(m)} = 0, 1, 2...N/4D$. In [57], the optimal shift values have been determined by using the variance of correlation (VC) of alternative OFDM signal sequences. The optimal shift values are indicated in Table 5.1. At last, four convoluted sequences are added. Therefore, the M alternative first-block OFDM signal $x_1^{(m,0)'}$ sequences are generated [57].

Let p^m be the u^{th} partial phase weighting conversion vectors to generate $x_1^{(m,0)'}$, which can be given by

$$p^{(m)} = \sum_{i=1}^{4} p_{i<\tau^{(m)}>}, \tag{38}$$

where $p_{i<\tau^{(m)}>}$ is the cyclic-shifted p_i to the right by $\tau^{(m)}$ samples. Hence, $x_1^{(m,0)'}$ is obtained by $x_1^{(m,0)'} = p^{(m)} \otimes_{N/D} x_1^{(0)'}$. It should be noted that the maximum number of optimal alternative OFDM signal sequences M is $N/8$ due to the variance between these shift values. The proof can be found in Ref. [57]. Therefore, in order to increase the number of candidate sequences, the "*conjugation theorem*" is applied, which is explained later.

After the time-domain partial phase weighting process, the sequence of the convo-

Table 5.1: Optimal Cyclic Shift Value

m	1	2	3	...	k
$\tau_1^{(m)}$	0	0	0	...	0
$\tau_2^{(m)}$	1	2	3	...	k mod $N/4$
$\tau_3^{(m)}$	2	4	6	...	$2k$ mod$N/4$
$\tau_4^{(m)}$	3	6	9	...	$3k$ mod $N/4$

luted first sub-block symbols can be obtained by applying the *"up-sampling theorem"*, which can be denoted as:

$$x_1^{(0,m)} = \frac{1}{D}[x_1^{(0,m)'}, ..., x_1^{(0,m)'}], \tag{39}$$

for $m = 1, \ldots, N/8$.

After the process of the time-domain partial phase weighting process, all the subblock sequences except the first subblock can be obtained by applying the *"circular shift theorem"*. The corresponding time-domain sequences can be obtained as follows:

$$\begin{aligned} x_2 &= x_2^{(1)}\mathbf{\Theta}W_{(1)} \\ x_3 &= x_3^{(2)}\mathbf{\Theta}W_{(2)} \\ &..... \\ x_D &= x_D^{(D-1)}\mathbf{\Theta}W_{(D-1)} \end{aligned} \tag{40}$$

where

$$W_{i-1} = \{1, \exp(j2\pi(i-1)/N), ..., \exp(j2\pi(i-1)(N-1)/N)\}, \quad i = 1, \ldots, N.$$

After all the time-domain subblock sequences are obtained, the candidate sequences can be generated by the combinations of all the time-domain subblock sequences.

In order to increase the number of candidate sequences, the conjugation property

of the IFFT is applied without increasing the number of complex multiplications. If the conjugation theorem is performed in the frequency-domain, the corresponding time-domain sequences can be generated from the original time-domain sequences. This way the number of additional IFFT operations can be reduced. Then applying to the "*conjugation theorem*", the conjugation operation is performed on X_2, X_3,...X_D one by one [54]. In this way, D more candidate sequences can be generated for each $x_1^{(0,m)}$. Therefore, the total number of candidate sequences in the proposed TPPW-SLM scheme becomes $D \times N/8$.

Finally, from all the possible candidates the one with the lowest PAPR is selected for transmission. The block diagram of the proposed TPPW-SLM scheme is shown in Fig. 5.1.

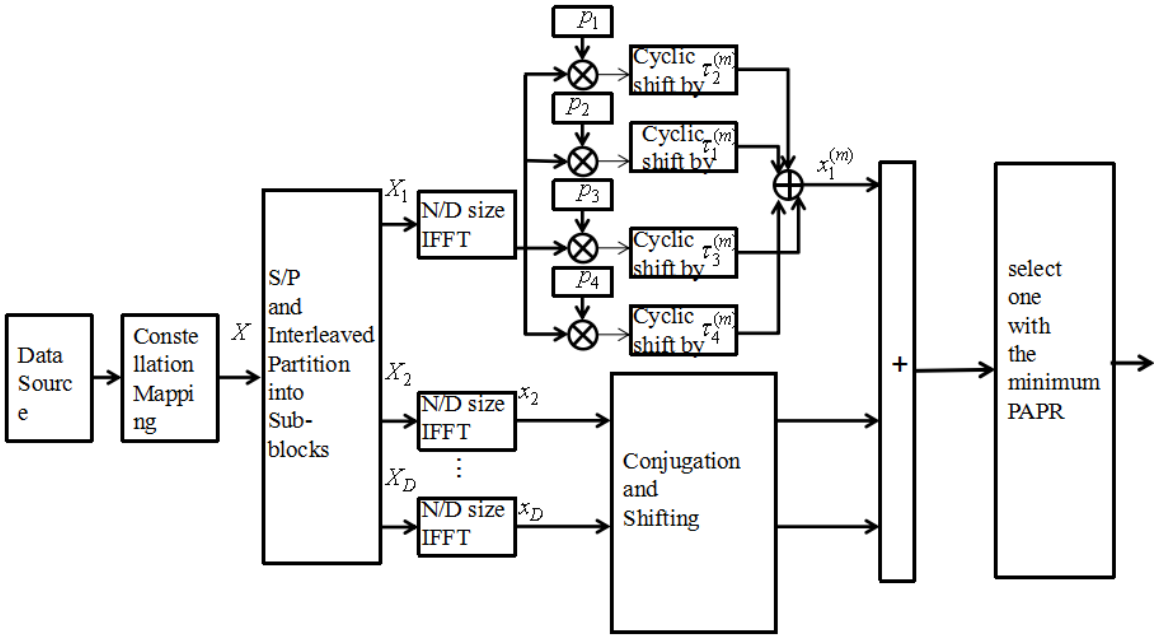

Fig. 5.1: Block diagram of the TPPW-SLM scheme.

Compared with the conventional SLM, the proposed TPPW-SLM does partial phase weighting for the first subblock in the time domain, which is essentially a kind of circular convolution and cyclic shifting. Moreover, by making use of the properties

of IFFT, the computational complexity of the proposed work can be further reduced. TPPW-SLM simplifies the calculation of IFFT whereas the FFT part at the receiver remains unchanged. Meanwhile, the side information is also required. Compared with the conventional SLM, the proposed scheme has the similar side information transmission scheme. For example, if there are U candidate sequences in the proposed scheme, thus, the number of required bits as side information is $\log_2 U$ bits for each block of data.

Note that the PAPR reduction performance is determined by the number of candidate sequences U. In the proposed TPPW-SLM scheme, the number of candidate sequences can be given by $U = D \times M$, where $1 \leq M \leq N/8$. Hence, the performance of the proposed TPPW-SLM scheme is governed by the number of partial phase weighted sequences M of the first subblock and the number of the subblocks D.

5.2.2 Computational complexity of TPPW-SLM

In this subsection, the computational complexity of the TPPW-SLM is determined and compared with various PAPR reduction schemes.

For the conventional SLM scheme, if it is assumed that the number of candidate sequences is U, the number of required IFFT units is U. It is known that an N-point IFFT operation requires $(N/2)\log_2(N)$ complex multiplications and $N\log_2(N)$ complex additions, where N is the number of points (or subcarriers in an OFDM signal). Hence the computational complexity of the conventional SLM is given as follows:

- the number of complex multiplications in C-SLM:

$$\frac{UN}{2}\log_2(N) \tag{41}$$

- the number of complex additions in C-SLM:

$$UN\log_2(N) \tag{42}$$

For the proposed TPPW-SLM scheme, its computational complexity is determined by the number of its IFFT operations, circular convolution for the first subblock, and the combinations of all the other subblock sequences for generating all the candidate sequences. The number of IFFT units is dominated by the number of subblocks D. However, the whole computational complexity of the IFFT operations is unchanged because the larger the number of subblocks is, the shorter the length of corresponding subblocks will be. For the first subblock, a total of $3N/D$ complex additions are involved in performing the circular convolution of x_1 with p_1, p_2, p_3, p_4. However, according to Ref. [20], only the first $N/4D$ points of the circular convolution are required. In addition, $3N/D$ complex additions are required to combine $x_1^{\tau_i}$, $i = 1, 2, 3, 4$. Hence, the total number of complex additions required for the first subblock to generate M candidate sequences is equal to $\frac{1}{D}LN\log_2(N/D) + \frac{3}{D}MN$. The other time-domain subblock signals can be achieved by *"circular shift theorem"* and *"up-sampling theorem"*, which require $(D-1)N/D[(1/2)\log_2(N/D) + (D+1)]$ complex multiplications and $(D-1)N/D[\log_2(N/D)]$ complex additions [54]. Since in the proposed scheme the subblock sequences are combined to generate the MD candidate sequences, the number of required complex additions is $MDN(D-1)$. However, some of additions in this process is trivial. For example, if $D = 4$, the linear combination of x_1^m, x_2, x_3 and x_4, as

$$x_1^m\mathbf{\Theta}W_{p0} + x_2^*\mathbf{\Theta}W_{p1} + x_3\mathbf{\Theta}W_{p2} + x_4\mathbf{\Theta}W_{p3}, \tag{43}$$

can be written as the following combination:

$$x_1^m \mathbf{\Theta} W_{p0} + [x_2 + (x_2^* - x_2)] \mathbf{\Theta} W_{p1} + x_3 \mathbf{\Theta} W_{p2} + x_4 \mathbf{\Theta} W_{p3}. \tag{44}$$

Now, the combination in (43) can be calculated from the following combination:

$$x_1^m \mathbf{\Theta} W_{p0} + x_2 \mathbf{\Theta} W_{p1} + x_3 \mathbf{\Theta} W_{p2} + x_4 \mathbf{\Theta} W_{p3}. \tag{45}$$

Calculating the difference part $(x_2^* - x_2)$ separately and substituting it along with (45) into (43) give (44).

Therefore, the additional complex additions for combination can be reduced to $M(2D-1)N$. Hence, when the number of subblocks is larger than one, the computational complexity of the proposed TPPW-SLM is given as follows:

- the number of complex multiplications in TPPW-SLM:

$$\frac{N}{2D}[D \log_2 \big(\frac{N}{D}\big) + D^2 - 1] \tag{46}$$

- the number of complex additions in TPPW-SLM:

$$N\big[\log_2 \big(\frac{N}{D}\big) + \frac{3}{D}M\big] + M(2D-1)(N) \tag{47}$$

Compared with PPW-SLM proposed by Lingyin. Wang and Ju. Liu in Ref. [54], the TPPW-SLM also shows advantages in terms of complexity reduction. According to Ref. [54], the complex multiplication and complex addition for PPW-SLM can be given as follows:

- the number of complex multiplications in PPW-SLM:

$$\frac{N}{D}[V^2 + D - 1 + \frac{1}{2}(V + D - 1) \log_2(\frac{N}{D})] \tag{48}$$

- the number of complex additions in PPW-SLM:

$$\frac{N}{D}[(V+D-1)\log_2(\frac{N}{D})+DV^2(V-1)] \tag{49}$$

where V is the number of phase rotation factors that are used by PPW-SLM in the first sub-blocks.

In order to make the comparison more understandable, the computational complexity reduction ratio (CCRR) is used to evaluate the computational complexity reduction of the TPPW-SLM against the conventional SLM (CSLM). The definition of the CCRR is given by

$$\text{CCRR} = 1 - (\frac{\text{Complexity of the proposed scheme}}{\text{Complexity of the conventional scheme}}) \times 100\% \tag{50}$$

Table 5.2 shows the computational complexity comparison between the TPPW-SLM and the CSLM, where the number of subcarriers N is 128. Moreover, the CCRR between TPPW-SLM and PPW-SLM is also compared in the table. In the PPW-SLM, the number of partial phase rotation factors V is set to 4. Fig. 5.2 is the corresponding CCRR figure that represents the CCRR of complex additions and complex multiplications with different number of subcarriers. For a fair comparison, all the schemes have the same number of candidate sequences.

It is shown in Fig. 5.2 that compared with the conventional scheme, the proposed TPPW-SLM scheme can significantly decrease computational complexity. It is worth noting that the performance of complexity reduction depends on the values of D and M such that the larger D is the more efficient the algorithm is in reducing the number of complex addition, while the larger M is the more efficient is in reducing the number of complex multiplications. Even the number of candidate signals of TPPW-SLM is doubled, the computational complexity of TPPW-SLM is still much less than that of the conventional SLM. In the case of $U = 8$,$M = D = 4$, the

Table 5.2: Comparison of computational complexity among CSLM, TPPW-SLM and PPW-SLM

Candidates	Calculation	TPPW-SLM	CSLM	PPW-SLM	$CCRR^{+}$	$CCRR^{*}$
U=16D=4M=4	Complex *	800	7168			88.8%
	Complex +	3973	14336		72.2%	
U=16D=2M=8	Complex *	576	7168			91.3%
	Complex +	4614	14336		67.8%	
U=8D=4M=4	Complex *	780	3584			79.8%
	Complex +	3239	7168		56.9%	
U=8D=2M=8	Complex *	573	3584			84.7%
	Complex +	3741	7168		49.9%	
D=M=V=4	Complex *		7168	4773		31.5%
	Complex +		14336	7264	45.3%	

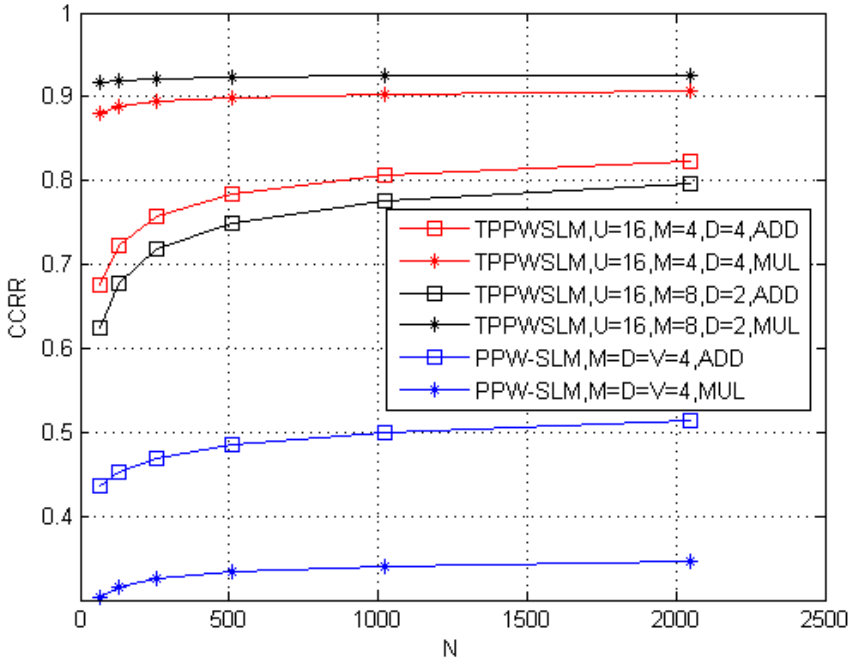

Fig. 5.2: CCRR performance comparison between the TPPW-SLM and the CSLM with the same number of candidate sequences.

proposed TPPW-SLM can still achieve 79.8% reduction in complex multiplications and 56.9% reduction in complex additions. Moreover, compared with the PPW-SLM proposed in Ref. [54], the TPPW-SLM also shows great advantages in computational complexity reduction. In the case of $V = M = D = 4$, the PPW-SLM can show 31.5%

reduction in complex additions and 45.3% in complex multiplications. This can be explained simply as follows: since in PPW-SLM, the first subblock is still rotated by phase rotation factors in the frequency domain, which still costs IFFT operations like the C-SLM, and the trivial additions of PPW-SLM in the process when combining all the subblock sequences also cause higher computational complexity.

5.2.3 Simulation results and analysis

According to the above section, the main idea of the proposed scheme has been introduced. In this part, the simulation results are performed and compared among the proposed TPPW-SLM scheme, the C-SLM, and the PPW-SLM scheme in Ref. [54]. The phase rotation factors are randomly taken from [1,-1]. In the simulation, the number of subcarriers are set to 128 and 256 respectively. The number of subblocks D are set to 2 and 4, respectively. The number of the candidate sequences in the first subblock are set to 8 and 4, and the number of partial phase rotation factors V in PPW-SLM is 4.

In Fig. 5.3, there are 16 candidate sequences generated in the proposed TPPW-SLM and PPW-SLM (i.e. $D = 4, M = 4$, $D = 2, M = 8$ and $D = 4, V = 4$), and 8 candidate sequences are generated in the C-SLM (i.e. $U = 8$). In the proposed TPPW-SLM, 16 candidate sequences can be generated with two different combinations of D and V ($D = M = 4$,$D = 2M = 8$). It is shown in the figure that, with the different number of candidate sequences, the performance of TPPW-SLM is better than that of C-SLM and similar as that of PPW-SLM. Although there are more complexities in the additions and the multiplications required, the computational complexity of the proposed TPPW-SLM with $M * D = 16$ is still much lower than that of CSLM with $U = 8$.

In Fig. 5.4, the number of candidate sequences of the TPPW-SLM, PPW-SLM and the CSLM are the same. The 16 candidate sequences of the TPPW-SLM can

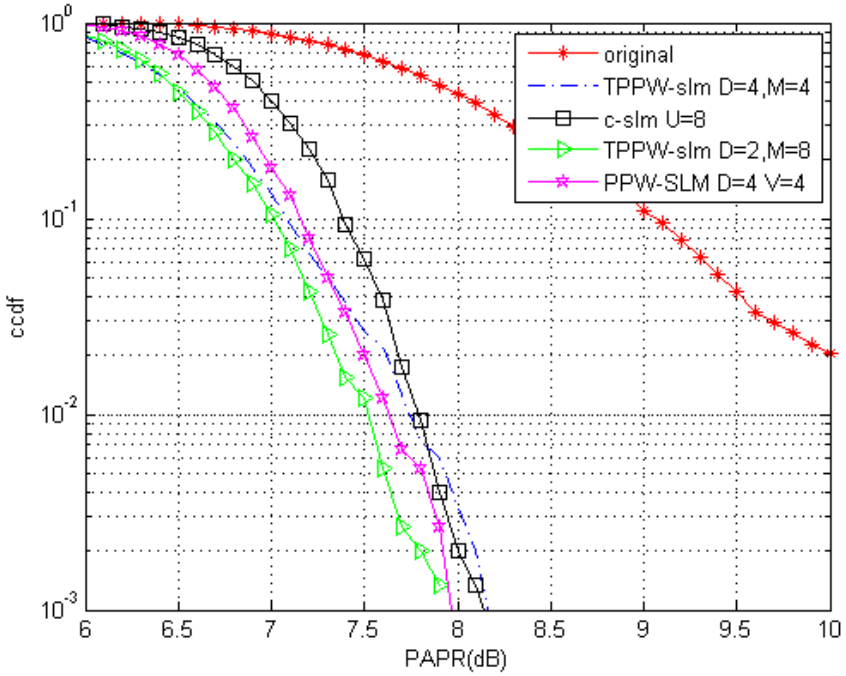

Fig. 5.3: CCDF performance comparison between CSLM and TPPW-SLM with different number of candidate sequences.

be generated in two ways (i.e. $D = M = 4, D = 2M = 8$). It is obvious that with the same number of candidate sequences, the PAPR reduction performance of the C-SLM is the best because of the higher randomness among its candidate sequences. Although PAPR reduction performance of the CSLM is better, the proposed SLM scheme can significantly reduce computational complexity with slightly degradation of PAPR reduction. In addition, the performance between TPPW-SLM and PPW-SLM are similar; however, the proposed TPPW-SLM shows more advantages in terms of computational complexity reduction than PPW-SLM.

In Fig. 5.5, the number of subcarriers are increased to 256. The C-SLM generates 8 candidate sequences, and both the proposed TPPW-SLM and PPW-SLM generate 16 candidate sequences. It can been seen from the figure that, compared with the C-SLM, the proposed SLM scheme can achieve better PAPR performance with lower computational complexity. Moreover, compared with the PPW-SLM, the proposed

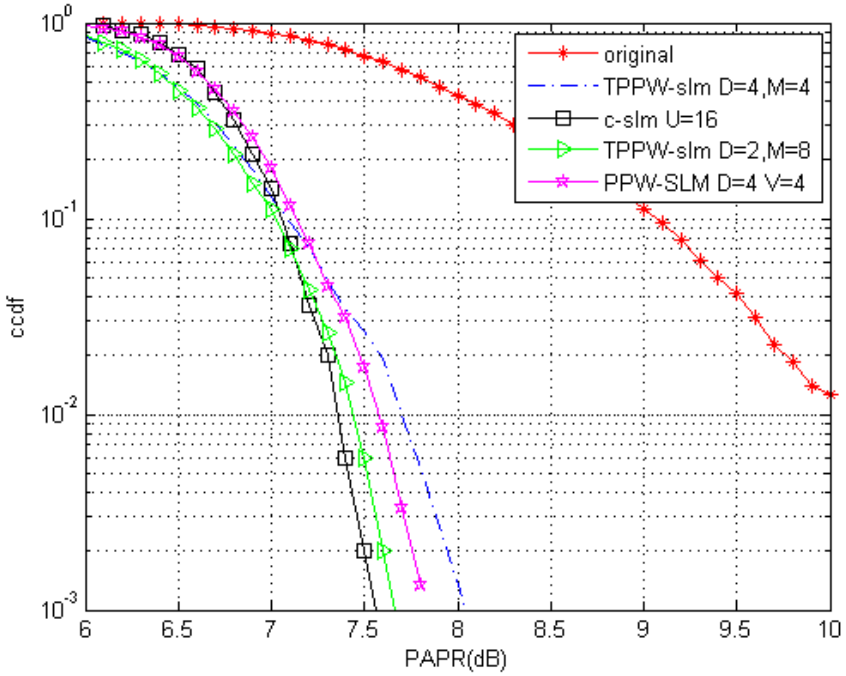

Fig. 5.4: CCDF performance comparison between CSLM and TPPW-SLM with the same number of candidate sequences.

TPPW-SLM can achieve similar PAPR reduction performance with lower complexity.

5.3 A novel partitioning and partial phase weighting SLM scheme

In this subsection, a new SLM scheme is proposed, which combines the advantages of low complex SLM with the advantages of low complex PTS. It is known that the conventional PTS scheme suffers from high computational complexity due to its exhaustive search [45]. In the proposed SLM scheme, a simplified PTS scheme using properties in phase rotation sequences is applied in order to decrease the computational complexity. Because the proposed scheme does not change the distance in constellation, the bit error rate (BER) is the same as that of the conventional SLM scheme. Moreover, the SI transmission scheme is still the same as that of conventional SLM.

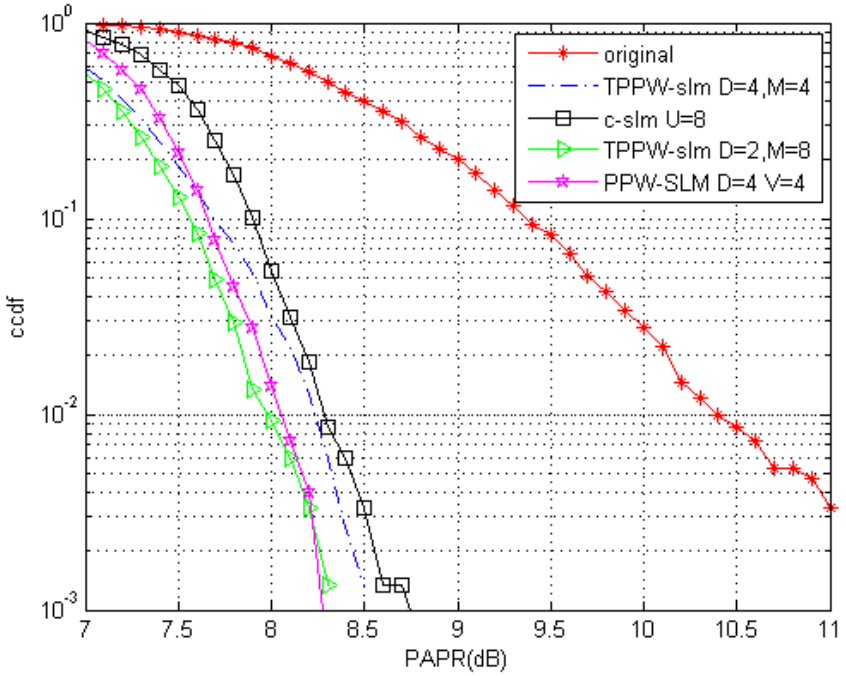

Fig. 5.5: CCDF performance comparison between CSLM and TPPW-SLM with different number of candidate sequences when N=256.

5.3.1 The main idea of the PPPW-SLM

In the proposed SLM scheme, first the input OFDM symbols X, with N subcarriers are partitioned into two kinds of subblocks. The first kind of subblock has half of the data and the rest of the data are partitioned into V disjoint subblocks by making use of the interleaving method [54], where V is a power of two. In this way, the input data can be written as follows:

$$X = X_0 + \sum_{i=1}^{V} X_i, \tag{51}$$

where X_0 is the first subblock, which has half of the data. All the subblocks can be given by

$$\begin{aligned}
X_0 &= [X_0, 0, X_2, 0, X_4, ..., X_{N-2}, 0], \\
X_1 &= [0, X_1, \underbrace{0, ...,}_{2V-1} X_{2V+1}, ..., 0, X_{N-2V+1}, ...0], \\
X_2 &= [0, ..., X_3 \underbrace{0, ...,}_{2V-1} X_{2V+2}, ..., 0, X_{N-2V+2}, ...0], \\
X_3 &= [0, ..., X_5, \underbrace{0, ...,}_{2V-1} X_{2V+3}, ..., 0, X_{N-2V+3}, ...0], \\
&..... \\
X_V &= [\underbrace{0, ...,}_{2V-1} X_{2V-1}, \underbrace{0, ...,}_{2V-1} X_{4V-1}, ..., \underbrace{0, ...,}_{2V-1} X_{N-1}].
\end{aligned} \tag{52}$$

Then, the system generates U' different phase rotation factors, which are statistically independent and used for weighing the first subblock, as

$$P^{(u')} = [p_0^{(u')}, 0, p_1^{(u')}, 0, p_2^{(u')}, ..., p_{N/2-1}^{(u')}, 0], \qquad u' = 0, \ldots, U', \tag{53}$$

where $p_i^{(u)} = \exp(j\varphi_i^{(u)})$, $\varphi_i^{(u)} \in [0, 2\pi)$, $i = 0, 1, ...(N/2) - 1$. In general cases, the phase rotation factors are taken randomly from a fixed set, such as $[-11]$ or $[1, -1, j, -j]$. It should be noted that only the first subblock is weighted at the first step, and the other subblocks stay unchanged until their corresponding time domain sequences are obtained.

After the process of phase rotation, all the subblocks (including the first U' phase weighted blocks and other subblocks) are transformed into the time domain through IFFT operations. Here, the first two properties of IFFT in section 5.1 are applied to make calculation simpler. They are executed as follows:

The *"up-sampling theorem"* is directly applied on the first subblock. After phase

rotation process, all rotated sequences in the frequency domain are expressed as:

$$X_0^{(u)} = [X_0 P_0^{(u)}, 0, X_3 P_1^{(u)}, 0, ..., 0, X_{N-2} P_{(N/2)-1}^{(u)}, 0].$$

Therefore, the time domain sequences $x_0^{(u)}, u = 1, 2, ..., U$ are given by

$$\begin{aligned} x^{(u')} &= \frac{1}{2}[\text{IFFT}\{X_0^{u'}\}, ..., \text{IFFT}\{X_0^{u'}\}], \\ &= \frac{1}{2}[\underbrace{x_0^{u'}, ..., x_0^{u'}}_{V}], \quad u' = 1, 2, ..., U, \end{aligned} \tag{54}$$

where $X_0^{(u)'} = [X_0 P_0^{(u')}, X_3 P_1^{(u')}, ..., X_{N-2} P_{(N/2)-1}^{(u')}, 0]$, and, $x_0^{(u)'} = \text{IFFT}\{X_0^{(u)'}\}$.

For the other subblocks, the time-domain sequences can be obtained by using *"circular shift theorem"* and *"up-sampling theorem"*. Since other subblocks $X_1, X_2, ...X_V$ are still temporarily unchanged, the subblock sequences are required to go through cyclic shifting first. The subblock sequences after cyclic shifting are written as follows:

$$\begin{aligned} X_1^{(1)} &= [X_1, \underbrace{0, ..., 0}_{2V-1}, X_{2V+1}, \underbrace{0, ..., 0}_{2V-1}, X_{N-2V+1}, \underbrace{0, ...0}_{2V-1}], \\ X_2^{(3)} &= [X_2, \underbrace{0, ..., 0}_{2V-1}, X_{2V+2}, \underbrace{0, ..., 0}_{2V-1}, X_{N-2V+2}, \underbrace{0, ..., 0}_{2V-1}], \\ &..... \\ X_V^{(2V-1)} &= [X_{2V-1}, \underbrace{0, ..., 0}_{2V-1}, X_{4V-1}, \underbrace{0, ..., 0}_{2V-1}, X_{N-1}, \underbrace{0, ..., 0}_{2V-1}], \end{aligned} \tag{55}$$

where $X_i^{(2i-1)}$, $i = 1, 2, ..., V$, represents $2i - 1$ elements of the i^{th} subblock sequence that is cyclically shifted to the left.

After cyclic shifting, using *"up-sampling theorem"*, the corresponding time-domain

sequences of subblocks are obtained directly, given by

$$\begin{aligned}
x_1^{(1)} &= \frac{1}{2V-1}[\underbrace{\text{IFFT}\{X_1^{(1)'}\}, ..., \text{IFFT}\{X_1^{(1)'}\}}_{2V-1}], \\
&= \frac{1}{2V-1}[\underbrace{x_1^{(1)'}, ..., x_1^{(1)'}}_{2V-1}] \\
x_2^{(3)} &= \frac{1}{2V-1}[\underbrace{\text{IFFT}\{X_2^{(3)'}\}, ..., \text{IFFT}\{X_2^{(3)'}\}}_{2V-1}], \\
&= \frac{1}{2V-1}[\underbrace{x_2^{(3)'}, ..., x_2^{(3)'}}_{2V-1}], \qquad (56) \\
&..... \\
x_V^{(2V-1)} &= \frac{1}{2V-1}[\underbrace{\text{IFFT}\{X_V^{(2V-1)'}\}, ..., \text{IFFT}\{X_V^{(2V-1)'}\}}_{2V-1}], \\
&= \frac{1}{2V-1}[\underbrace{x_V^{(2V-1)'}, ..., x_V^{(2V-1)'}}_{2V-1}],
\end{aligned}$$

where

$$X_i^{(2i-1)'} = [X_i, X_{2V+i}, ..., X_{N-2V+i}],$$

$x^{(2i-1)} = \text{IFFT}\{X_i^{(2i-1)'}\}$, for $i = 1, 2, ..., V$. Equation (28) about circular shifting can be directly adopted for all the subblock sequences except the first one. The time-domain sequences can be denoted as follow:

$$\begin{aligned}
x_1 &= x_1^{(1)} \mathbf{\Theta} W_{(1)}, \\
x_2 &= x_2^{(3)} \mathbf{\Theta} W_{(3)}, \\
&..... \\
x_V &= x_V^{(2V-1)} \mathbf{\Theta} W_{(2V-1)},
\end{aligned} \qquad (57)$$

where

$$W_i = \{1, \exp(j2\pi i/N), ..., \exp(j2\pi i(N-1)/N)\}, \quad \text{for } i = 1, ..., N.$$

After all the time-domain subblock sequences are obtained, the subblock sequences, except the first one, are optimized by phase rotation factors $b_i, i = 1, 2, ...V$, which is similar as that in PTS. However, the phase optimization usually has high computational complexity in the conventional PTS because it requires an exhaustive search to obtain a combination of optimized phase rotation factors. In the proposed scheme, a low computational complexity way is implemented by using the inner-relationship between different phase rotation factors.

Since the first subblock stays unchanged when other subblocks going through phase optimization, this subsection is only concentrated on the rest of V disjoint subblocks. After phase optimization, the first subblock sequences that are weighted by different phase rotation factors are combined to obtain more candidate sequences.

Specifically, the number of V disjoint subblocks $X_i, i = 1, 2...V$ are passed through IFFT operations according to the above properties of the IFFT. By applying a phase weighting factor $b_i, i = 1, 2, ...V$, alternative time-domain signal sequences are given by

$$x' = \text{IFFT}\{\sum_{i=1}^{V} b_i X_i\} = \sum_{i=1}^{V} b_i \text{IFFT}\{X_i\} = \sum_{i=1}^{V} b_i x_i. \tag{58}$$

In order to reduce the complexity of the proposed scheme, the first phase weighting factor in PPPW-SLM, which is applied to the second subblock, is set 1. To obtain the optimal phase weighting factors, W^{V-1} , where W is one of the factors in sets (such as $[-1, 1]$ for $W = 2$), all the combinations must be checked, and then the best sequence with the minimum PAPR is transmitted. The exhaustive optimization requires a large number of complex multiplications and additions, which increase the computational intricacy.

It is observed that in the corresponding positions of any two sequences from all the phase weighting sequences, some phasing factors are opposite and the rest ones are the same, [44].

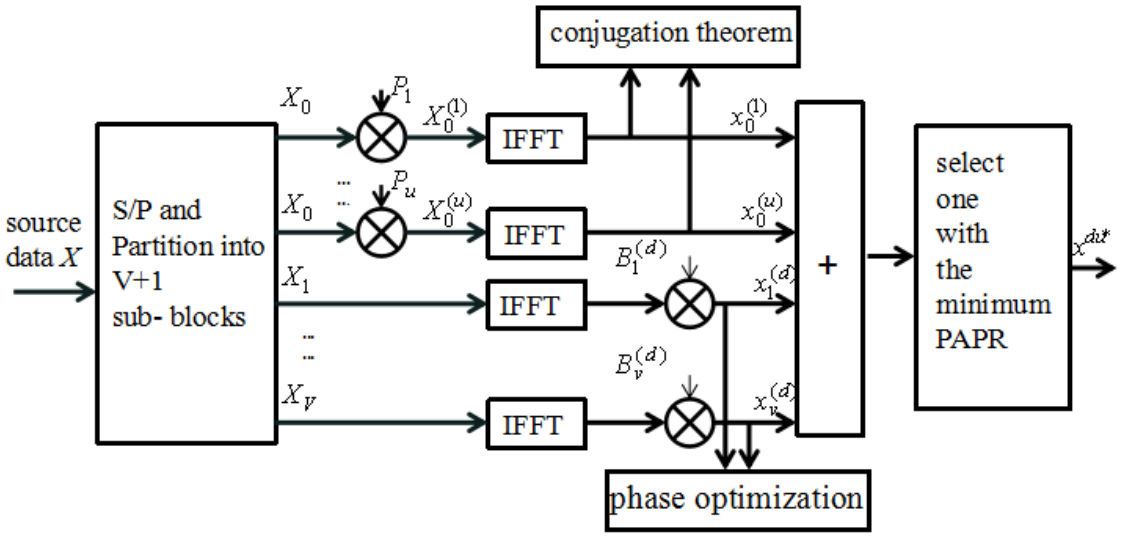

Fig. 5.6: Block diagram of the PPPW-SLM.

For example, when the number of subblocks is 4 and the phase rotation factors are chosen from the set $\{-1, 1\}$, all the weighting factors, denoted by $B^{(d)}$, are shown in Table 5.3.

Table 5.3: All the phase rotation factors for V=4

	phase weighting sequences		phase weighting sequences
B_1	[1 1 1 1]	B_5	[1 -1 -1 -1]
B_2	[1 1 1 -1]	B_6	[1 -1 -1 1]
B_3	[1 1 -1 1]	B_7	[1 -1 1 -1]
B_4	[1 1 -1 -1]	B_8	[1 -1 1 1]

A conclusion from Table 5.3 can be obtained that all the phase factors except the last position are the same in the corresponding digit positions of B_1, B_2, and the same story happens in other groups, which are B_3 and B_4, B_5 and B_6, B_7 and B_8.

In [44], one method has been proposed based on such observations. In this research, all the phase factors are divided into two parts first. Then, one of the two parts is chosen to be divided into a number of troops further, [44]. This way, the

common term just needs to be calculated once by making use of the inner relationship among those candidate sequences. As for the sequences in different parts, the common terms for generating candidate sequences in the other part can be obtained, which results in the fact that candidates in the other part can be directly calculated by complex additions. The specific steps are as follows:

1. Generate all phase rotation factors B_i, $i = 1, ...V$ from the set $\{1, -1\}$ or $\{1, j, -1, -j\}$. It should be noted that the assumption of using the set $\{1, -1\}$ or $\{1, j, -1, -j\}$ is only for simplicity and does not exclude any other sets.

2. Split the phase rotation factors into two parts with equal number of elements. For any two phase rotation sequences in each part, the second elements should be the same.

3. Choose any one of the two parts and divide into several troops, where the sequences with the same elements on the second position should be in the same troop, and then continue splitting each troop into smaller troops, where the sequences with the same elements on the third position should be in the same troop. After $V - 2$ times of splitting, each troop has W phase weighting factors (for example: if the set is $\{1, -1\}$, then $W = 2$). The last dividing step is to put the rotation factors, which have the opposite element on the last position, in the same troop. Finally, each troop only has two weighting sequences, where the relationship of these two sequences is that all phase weighting factors except the last elements are the same in the corresponding positions [44].

4. For each troop, candidate sequences can be calculated in an easy way by making use of the inner relationship between two weighted sequences. Furthermore, when the relationship between two sequences in different troops is considered, it is indicated that they have the same first element and opposite other elements:

$S_i = y_i - x_1$, $i = 1, 2, ..., W^{V-1}$, where y_i is the candidates in the selected part and x_1 is the first subblock sequence.

5. The candidate sequences can be directly generated by using the common parts in step (4).

To make the above explanation easier to understand, the given sequences in Table 5.3 are used as an example. First, all phase rotation factors in Table 5.3 are divided into two parts, where each column is one part. Then, one part, for example the first column, is selected. According to step (3), the final divided results can be given as B_3 and B_4, B_1 and B_2, where the first three phase elements are the same and the last digit is opposite. After that, the candidates y_1 and y_2 can be obtained from B_1 and B_2 as follows:

$$\begin{aligned} y_1 &= x_1 + \sum_{i=2}^{3} b_{1,i} x_i + b_{1,4} x_4, \\ y_2 &= x_1 + \sum_{i=2}^{3} b_{1,i} x_i - b_{1,4} x_4. \end{aligned} \tag{59}$$

First, the common parts $\sum_{i=2}^{3} b_{1,i} x_i$ and $b_{1,4} x_4$ can be obtained, and then y_2 can be easily calculated from the above relationship, which requires only N complex additions instead of $(V-1)N$ additions and $(V-1)N$ complex multiplications. Then, y_3 and y_4 can be calculated in the same manner from the relationship between B_3 and B_4. By considering the phase rotation from different parts, since $b_{i,k} = b_{i+4,k}$ and $b_{i,k} = -b_{i+4,k}$, for $i = 1, 2, 3, 4$, $k = 2, 3, 4$, the same terms in those sequences can be found, which is $S_i = y_i - x_i$, $i = 1, 2, 3, 4$. Therefore, candidate sequences in the other parts can be obtained according to this relationship only through complex additions,

given by

$$\begin{aligned} B_5 : y_5 = x_1 - S_1; \quad B_6 : y_6 = x_1 - S_2; \\ B_7 : y_7 = x_1 - S_3; \quad B_8 : y_8 = x_1 - S_4. \end{aligned} \tag{60}$$

This way, all the candidate sequences are obtained.

After combining the subblock sequences X_i, $i = 0, 1, 2..., V$ with the phase rotated subblock $X_0^{(u')}$, $u' = 1, 2..., U'$, the sequence with the lowest PAPR is selected and transmitted. The block diagram of the proposed scheme is given by Fig. 5.6.

It is should be noted that, if U' phase rotation factors are taken for the first subblock, there will be $U'W^{V-1}$ number of candidate sequences, where W is the number of factors in the set (for example, $W = 2$ if phase rotation factors of the other subblocks are selected from $\{1, -1\}$, which is large enough if V is greater than 2. Furthermore, the *"conjugation theorem"* of IFFT can be used to generate more number of candidate sequences by using more complex additions; however, because the above process has generated enough number of candidate sequences, there is no need to use *"conjugation theorem"* to generate more sequences. Therefore, more details about the PPPW-SLM scheme with conjugation theorem are not discussed, but the principles of the PPPW-SLM with conjugation theorem are the same as this scheme without adopting such theorem.

5.3.2 Computational complexity of the PPPW-SLM

In this subsection, the computational complexity of the proposed PPPW-SLM and the conventional SLM is determined. In order to make comparisons more understandable. the computational complexity of IFFT operations and phase optimization are discussed ,respectively.

On the one hand, it is well known that if the conventional SLM (CSLM) has U candidate sequences, it will take U IFFT operations. For each N-point IFFT oper-

ation, $(N/2)\log_2(N)$ complex multiplications and $N\log_2(N)$ complex additions are required, where N is the number of subcarriers. Hence, in the CLSM, the complexity of computation in IFFT and phase rotation process is indicated as follow:

- the number of complex multiplications in CSLM:

$$\frac{UN}{2}\log_2(N) \tag{61}$$

- the number of complex additions in PPPW-SLM:

$$UN\log_2(N) \tag{62}$$

On the other hand, in the proposed SLM scheme (PPPW-SLM), the number of IFFT is determined by the number of phase rotation factors for subblock X_0 , denoted by U', the number of other subblocks, denoted by V. The weighted first block requires $\frac{U'N}{2}[\frac{1}{2}\log_2(\frac{N}{2}+1)]$ numbers of complex multiplications and $\frac{U'N}{2}\log_2(\frac{N}{2})$ numbers of complex additions. The other time domain subblocks sequences before phase optimization can be obtained from the IFFT properties, which requires $\frac{(V-1)N}{2V}[\log_2(\frac{N}{2V})+(V+1)]$ times of complex multiplications and $\frac{(V-1)N}{2V}\log_2(\frac{N}{2V})$ numbers of complex additions [54]. Moreover, complex multiplications and complex additions still need to be performed when the other subblocks are going through the phase optimization process, where $\frac{N}{4}(V-1)2^{(V-1)}$ numbers of complex multiplications and $(1+\frac{V}{4})N2^{(V-1)}$ numbers of complex additions are required [44]. Finally, in order to add all subblocks up, additional $2^{V-1}U'N$ complex additions are required. Hence, for the PPPW-SLM:

- the number of complex multiplications in PPPW-SLM:

$$\frac{U'N}{4}\log_2(\frac{N}{2})+\frac{(V-1)N}{2V}\log_2(\frac{N}{2V})+\frac{V}{4}(V-1)2^{(V-1)} \tag{63}$$

- the number of complex additions in PPPW-SLM:

$$\frac{U'N}{2}\log_2(\frac{N}{2}) + \frac{(V-1)N}{2V}\log_2(\frac{N}{2V}) + [(1+\frac{V}{4})N + U'N]2^{(V-1)} \tag{64}$$

Fig. 5.7 and Fig. 5.8 show the additive CCRR and multiplicative CCRR of PPPW-SLM over CSLM with the same and different number of candidate sequences. For the proposed scheme, the different combinations of the number of phase rotation factors U' and the number of subblocks V are considered. As seen in Table 5.4, the PPPW-SLM can significantly reduce computational complexity. For instance, in the case of $U = 16, N = 128$, the complexity reduction of multiplications can reach to 81.2% when $U' = 2, V = 4$ and the complexity reduction of additions can reach to 66.3% when $U' = 8, V = 2$.

Additionally, in PPPW-SLM, even more candidate sequences are generated in order to achieve better PAPR reduction performance. The proposed PPPW-SLM can still reduce computational complexity compared with CSLM. Fig. 5.8 shows the additive CCRR and multiplicative CCRR of PPPW-SLM over CSLM with the double number of candidate sequences. Moreover, according to Table 5.4, in the case of $U = 8, N = 128$, the proposed PPPW-SLM can still achieve 62.4% reduction for complex additions reduction when $U' = 8, V = 2$ and 32.7% reduction for complex multiplications when $U' = 2, V = 4$.

For the proposed PPPW-SLM scheme, the PAPR reduction performance can be dominated by the number of candidate sequences. However, the number of candidate sequences can be combined by different U' and V. The above two figures show that by increasing V and decreasing U' the complexity can be reduced more.

Table 5.4: Comparison of computational complexity between CSLM and PPPW-SLM.

Candidates	Calculation	PPPW-SLM	CSLM	$CCRR^{+}$	$CCRR^{*}$
U=16V=2U'=8	Complex *	1765	7168		75.3%
	Complex +	4820	14336	66.3%	
U=16V=4U'=2	Complex *	1354	7168		81.2%
	Complex +	4721	14336	67.1%	
U=8V=2U'=8	Complex *	1765	3584		50.7%
	Complex +	4820	7168	32.7%	
U=8V=4U'=2	Complex *	1354	3584		62.4%
	Complex +	4721	7168	34.1%	

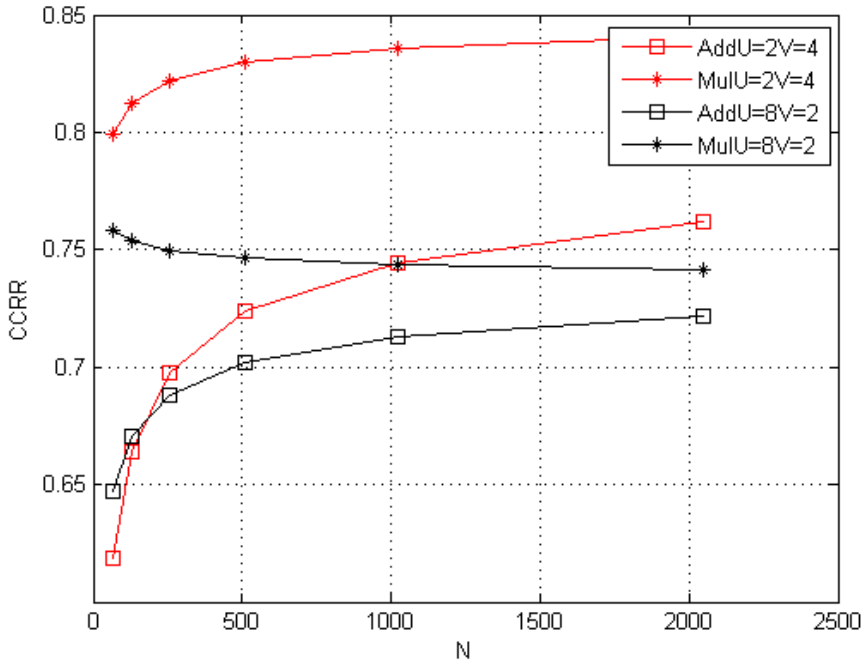

Fig. 5.7: CCRR performance comparison between PPPW-SLM and CSLM, U=16.

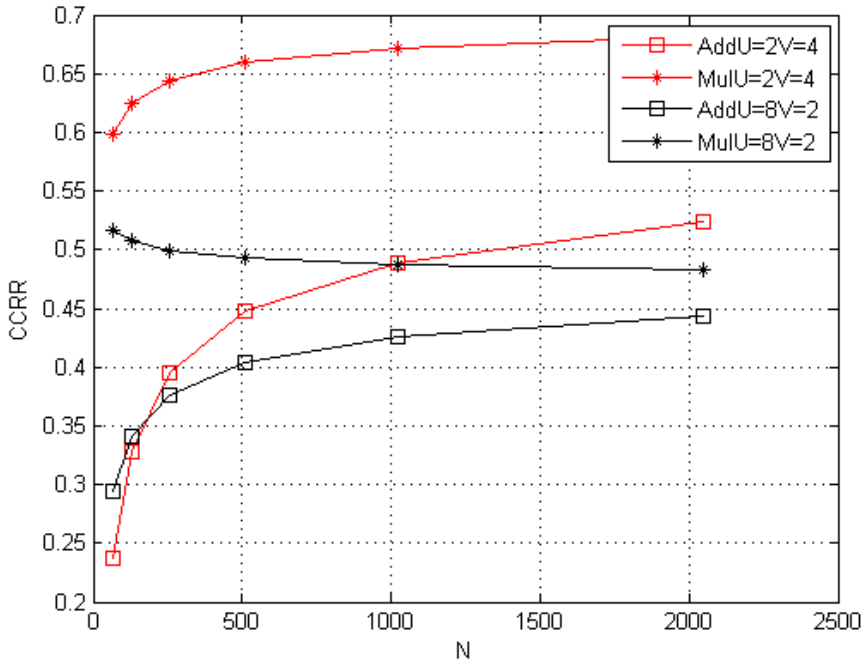

Fig. 5.8: CCRR performance comparison between PPPW-SLM and CSLM, U=8.

5.3.3 Simulation results

In this subsection, all the simulation results are analyzed. In order to compare the PAPR reduction performance, the CCDF of the PPPW-SLM scheme is evaluated. For the CSLM and PPPW-SLM, the PAPR performance is dominated by the number of candidate sequences, which are the combinations of V and U'. More candidate sequences means more selections for the system, and it has higher possibility to pick up a sequence with lower PAPR. In these simulations, the OFDM system has 128 or 256 subcarriers ($N = 128$ or $N = 256$) with 16-QAM constellation, and no conjugation process is used for simplicity. However, it should be expected that the conjugation process will generate more candidate sequences, which can improve the PAPR reduction performance with a minor complexity increase. The elements of phase rotation factors are randomly taken from $[+1, -1]$, which means $W = 2$ in the phase optimization process.

The PAPR reduction performance is compared in Fig. 5.9, Fig. 5.10, Fig. 5.11 with the same number of candidate sequences, different number of candidate sequences, or different number of subcarriers N, respectively. It can be shown from these figures that the PPPW-SLM can greatly reduce the PAPR compared with the original signal, and the performance is close to that of the CSLM, with 0.5dB loss at most. However, the computational complexity of the PPPW-SLM is significantly reduced compare with that of the CSLM.

In Fig. 5.9, 16 candidate sequences are generated by both CSLM scheme and PPPW-SLM scheme. For the proposed SLM scheme, two different combinations that can obtain 16 candidate sequences are compared, that is $V = 4, U' = 2$ and $V = 2, U' = 8$. It is shown that with the same number of candidate sequences, the CSLM has the best performance. It is because in the CSLM, the original sequence is rotated one by one but in the proposed SLM scheme, the sequence is rotated in groups except the first subblock. However, the slight degradation of PAPR reduction performance is at the cost of improving the computational complexity reduction performance.

Moreover, in order to improve the PAPR reduction performance, more candidate sequences in the PPPW-SLM scheme are generated. In Fig. 5.10, the number of candidate sequences in the CSLM is 8, and the number of candidate sequences in the PPPW-SLM is 16. As seen in 5.10, by increasing the number of candidate sequences, the PAPR reduction performance of the PPPW-SLM becomes better. In the case of $V = 4, U' = 2$, the PAPR reduction performance is better than that of the CSLM, and in the case of $V = 2, U' = 8$, the performance is the same as that of CSLM. Although more candidate sequences require more complex multiplications and complex additions, the computational complexity of PPPW-SLM is still much less than that of CSLM, which is shown in Fig. 5.8 and Table 5.4.

Fig. 5.11 shows that with the increase of the number of subcarriers, the PAPR reduction performance gap becomes larger compared with the case where $N = 128$. In

the case of $V = 4, U' = 2$, the gap between PPPW-SLM and CSLM is close to 0.3dB. It is because when $N = 256$, the subblocks have more elements that need to be rotated in groups, which means less randomness the candidate sequences have. Further, less randomness among candidate sequences causes PAPR reduction performance degradation. However, Fig. 5.7 and Fig. 5.8 show that the computational complexity decrease significantly as the number of subcarriers N increases.

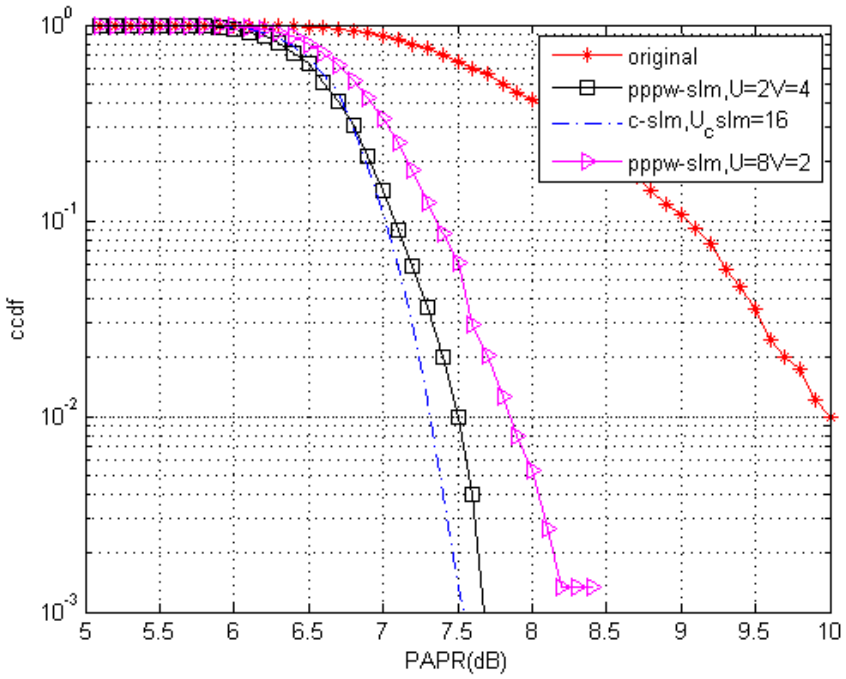

Fig. 5.9: CCRR performance comparison between PPPW-SLM and CSLM with the same number of candidate sequences.

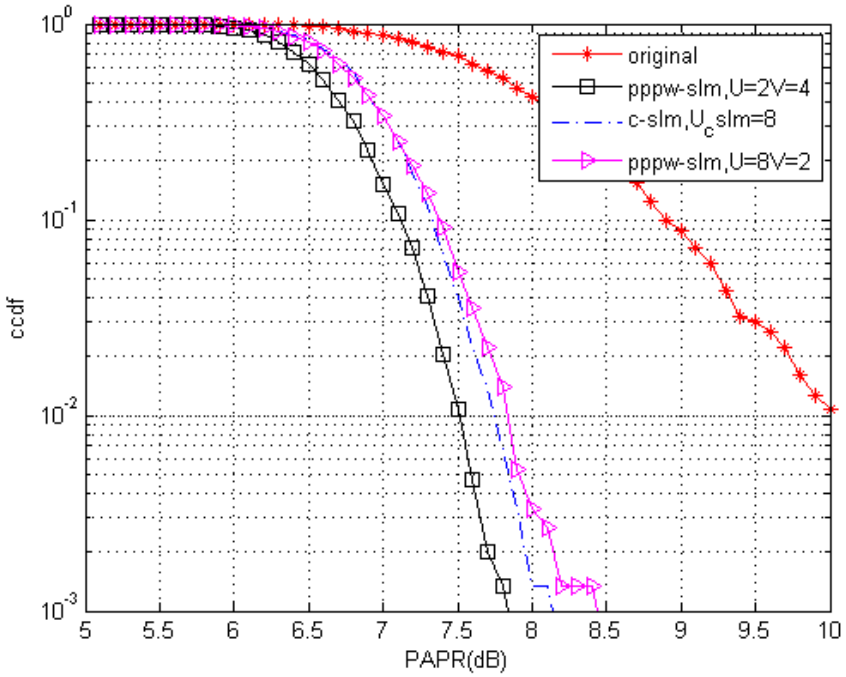

Fig. 5.10: CCRR performance comparison between PPPW-SLM and CSLM with different number of candidate sequences.

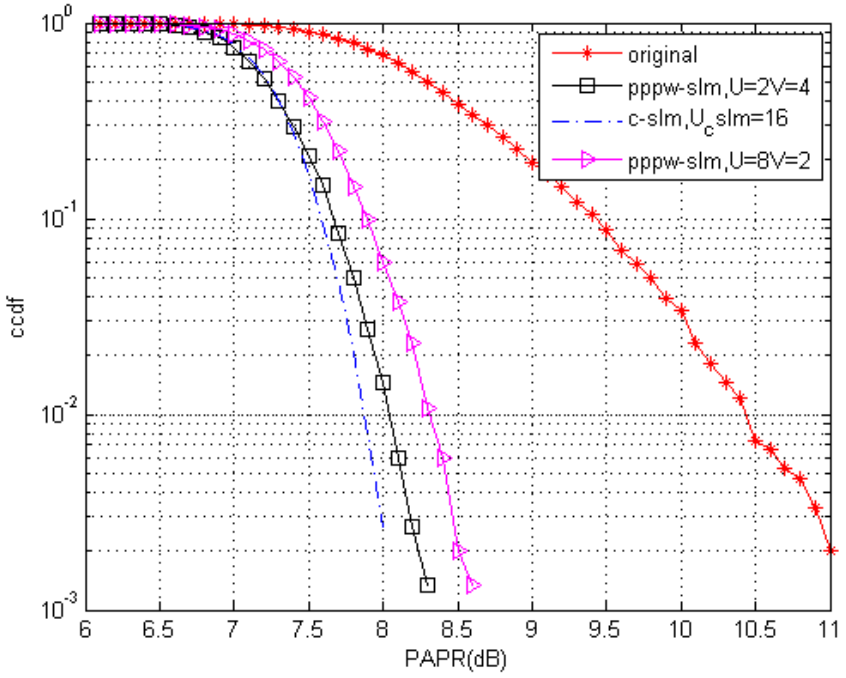

Fig. 5.11: CCRR performance comparison between PPPW-SLM and CSLM when N=256.

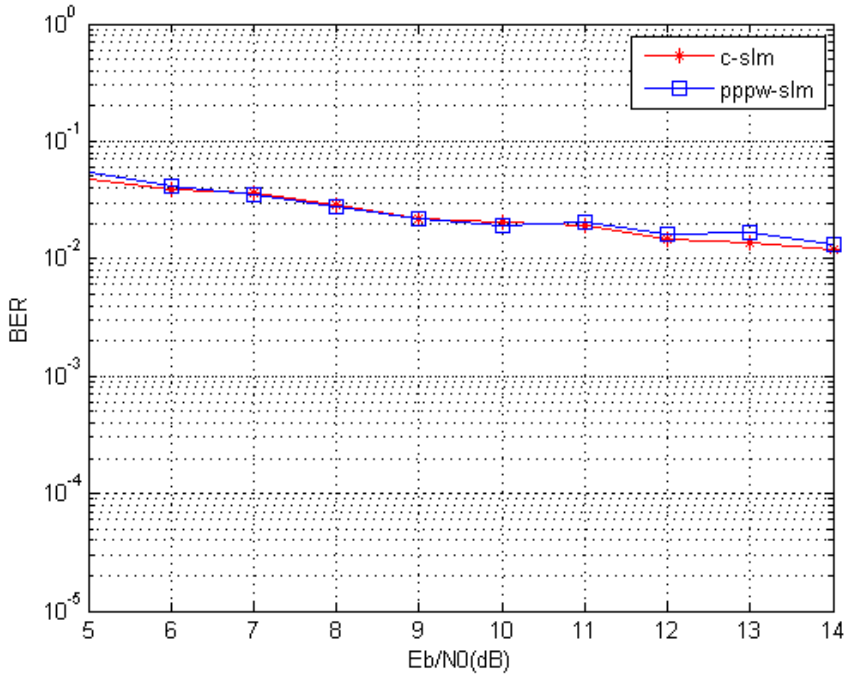

Fig. 5.12: BER performance comparison between PPPW-SLM and CSLM over the AWGN channel.

Now, the BER performance of the proposed PPPW-SLM is introduced briefly. Because the proposed PPPW-SLM scheme does not change the minimum distance in constellation, and does not distort the signal. The BER of the pppw-slm should be expected to be the same as that of the CSLM. Fig. 5.12 is the BER performance of the two schemes in AWGN channels.

5.4 A low complex SLM with signal construction scheme and fewer IFFT operations for PAPR reduction of QAM-OFDM signals

In this subsection, a new SLM scheme with low complexity is proposed. The proposed scheme requires only two FFT operations and achieves effective PAPR reduction performance with no addition side information compared to the conventional SLM. The new scheme outperforms the existing Class-III SLM scheme, [20], [57], in terms of

PAPR reduction performance. In this proposed scheme, the number of candidate sequences increases by forming a 16-QAM signal construction before circular convolution.

5.4.1 The main idea of the proposed SLM scheme

In this subsection, a new SLM scheme that combines M-QAM construction with the time domain circular convolution is proposed for PAPR reduction.

Fig. 5.13 shows a block diagram of the proposed SLM scheme. It is clear that only two IFFT operations are required in the proposed scheme. Now consider $X = [X_0, X_1, X_2, ...X_N - 1]$ as the input symbols that are modulated by QPSK. After S/P conversion, the original X are divided into two groups as X_1 and X_2 in order to construct different 16-QAM signals. In order to show that two QPSK signals can form a set of new 16-QAM signals. one example is given where X_1 and X_2 are QPSK signals, which belong to $\frac{1}{\sqrt{N}}\{1+j, 1-j, -1+j, -1-j\}$. The 16-QAM signal can be constructed by combing X_1 and X_2 in the specific steps shown in Fig. 5.13, [55].

Now the signal X is defined as follows:

$$X = a_1 X_1 + a_2 X_2 \tag{65}$$

where by selecting proper a_1 and a_2, a 16-QAM signal can be constructed, [55]. For example, if X_1 is quaternary 0, $a_1 = \sqrt{2}$ and $a_2 = 2\sqrt{2}\exp(j\pi k/2)$, where $k = 0, \ldots, 3$. In this case, according to (65), independent of X_2, X will fall into the 16-QAM constellation, which is in the circle group shown in Fig. 5.14. Also, if X_1 is quaternary 1,2, or 3, X certainly falls into the square, triangle or octagon group, [55]. Since the frequency-domain superposition can be replaced by the time-domain linear superposition after IFFT operations, we can generate the time domain signal using

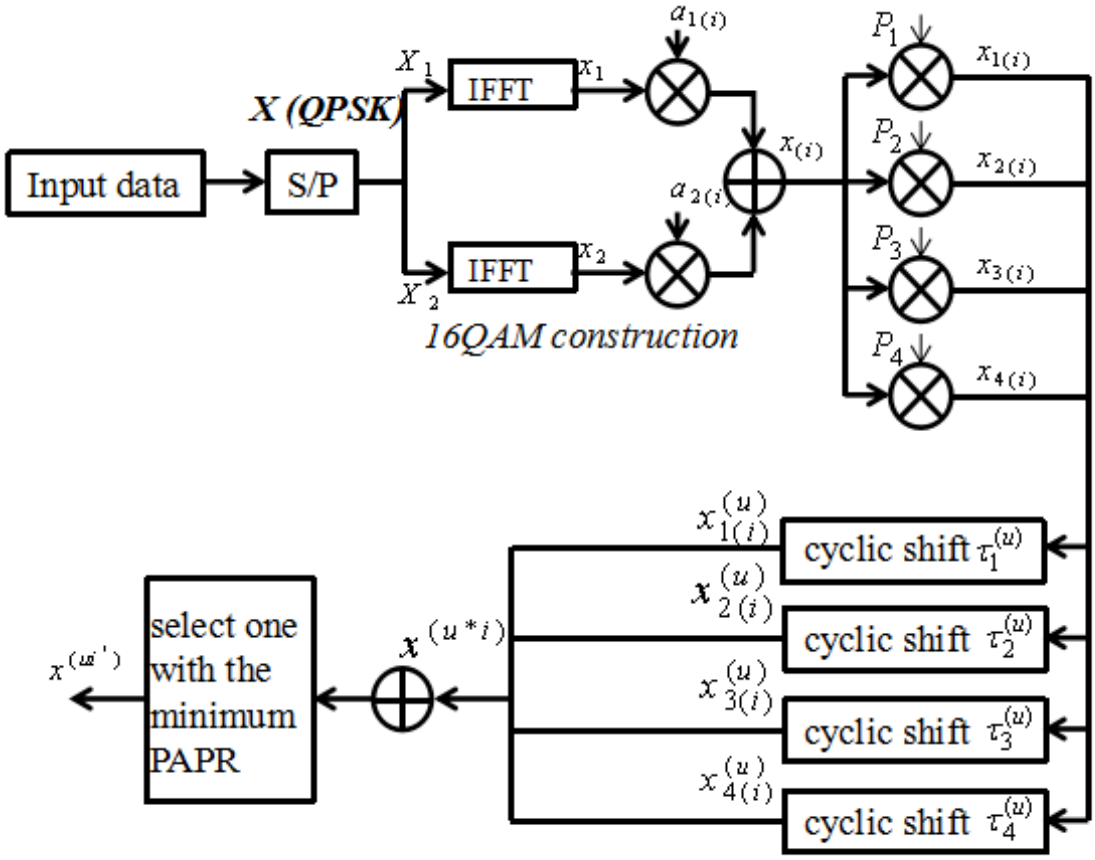

Fig. 5.13: The proposed SLM scheme.

the following equation:

$$x = a_1 x_1 + a_2 x_2. \tag{66}$$

One thing should be noted is that some of those X could have the same energy even different a are selected. For example, if X_1 and X_2 are fixed, the PAPR for $a_1 = \sqrt{2}\exp(0)$, $a_2 = 2\sqrt{2}\exp(0)$ and, $a_1 = \sqrt{2}\exp(j\pi/2)$, $a_2 = 2\sqrt{2}\exp(j\pi/2)$ are the same. Therefore, the following steps are used to avoid such cases [55]:

1. Let $a_1 = \sqrt{2}$ and choose a_2 from $2\sqrt{2}\exp(j\pi k/2)$, $k = 0, 1, 2, 3$ randomly, thus the system generates 4 16-QAM signal candidates that are unique.

2. Let $a_1 = 2\sqrt{2}$ and choose a_2 from $\sqrt{2}\exp(j2\pi k/2)$, $k = 0, 1, 2, 3$. In this way,

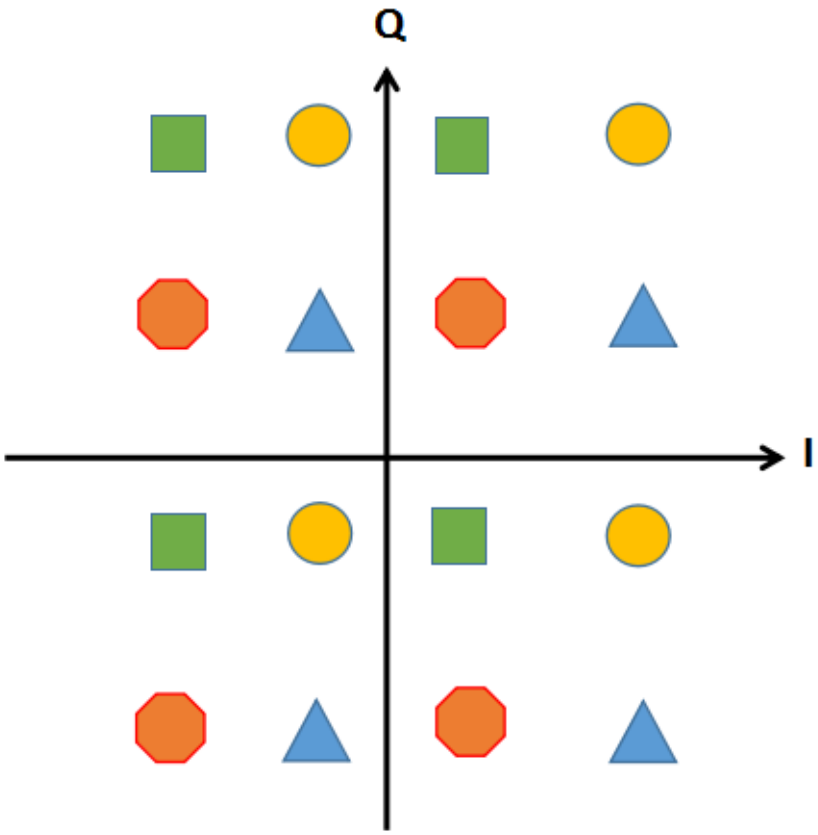

Fig. 5.14: 16-QAM constellation.

the system generates 4 other different 16-QAM signals.

As a result, 8 different 16-QAM signals with different PAPR can be obtained by using just 2 QPSK signals and 2 IFFT operations.

After 16-QAM signal generation, the circular convolution process in Ref. [20] is performed. The circular convolution process is the same as that in TPPW-SLM scheme, which was given in section 5.2.

In the proposed scheme, because the 16-QAM construction scheme is applied before convolution, more candidate sequences can be provided than that of pure circular convolution, which is used in Class-III SLM scheme [57]. Therefore, with increasing the number of candidate sequences, the probability of finding a candidate sequence with lower PAPR increases. In the proposed SLM scheme, $(N/8) \times 8 = N$

candidate sequences can be generated with an additional IFFT operation.

5.4.2 Computational complexity analysis on the proposed SLMl

In this section, the overall computational complexity for the conventional SLM (C-SLM) and proposed SLM (called p-SLM) schemes are compared.

It is well known from the literature that a N-point FFT requires $(N/2)\log_2(N)$ complex multiplications and $N\log_2(N)$ complex additions. Therefore, the C-SLM with M candidates requires $(MN/2)\log_2(N)$ complex multiplications and $(MN)\log_2(N)$ complex additions, respectively. First, the p-SLM scheme requires two IFFT operations, which take $(N/2)\log_2(N/2)$ complex multiplications and $N\log_2(N/2)+8N$ complex additions to generate 8 different 16-QAM signals [55], which contain the same information as that of 2 QPSK signals. After higher-order modulation signal construction, $3N$ complex additions are involved in performing the circular convolution of X with P_i, where $i = [1, 2, 3, 4]$. However, according to Ref. [20], only the first $N/4$ points of convolutions are needed. Hence, $3N/4$ complex additions are required to perform the circular convolution, where $i = 1, \ldots, 8$, $u = 1, \ldots, N/8$. Therefore, for 8 different 16-QAM signals which is constructed by 2 specific QPSK signals, if U' candidate sequences are generated for each 16-QAM sequence, where $U' \leq N/8$, $N\log_2(N/2) + 3U'N/2$ additional complex additions are required. Hence, the proposed SLM scheme totally requires $(N/2)\log_2(N/2)$ complex multiplications and $DN + (3DU'N/2) + N\log_2(N/2)$ complex additions, where D is the number of 16-QAM signals that are generated by combing QPSK signals after IFFT operations. It should be noted that in our proposed SLM scheme, the maximum number $D = 8$, $U' = N/8$ and the maximum number of candidate sequences is N.

Fig. 5.15 shows the CCRR performance of the p-SLM scheme and the Class-III-SLM scheme in Ref. [20], and the C-SLM scheme with different number of subcarriers N, where mul is short for "complex multiplication" and add is for "complex addi-

Table 5.5: CCDR performance Comparison of three schemes: CSLM, p-SLM and Class-III SLM.

Candidates	Calculation	p-SLM	CSLM	ClassIII-SLM	$CCRR^{+}$	$CCRR^{*}$
M=16D=2U'=8	Complex *	768	7168			88.9%
	Complex +	4096	14336		71.4%	
M=16D=4U'=4	Complex *	768	7168			88.9%
	Complex +	4253	14336		70.3%	
M=8D=2U'=8	Complex *	768	3584			77.8%
	Complex +	4096	7168		42.8%	
M=8D=4U'=4	Complex *	768	3584			77.8%
	Complex +	4253	7168		40.6%	
U=M=16	Complex *		7168		896	87.5%
	Complex +		14336	6592	54.0%	

tion". In order to keep fairness and show the advantages of the proposed SLM scheme at the same time, value M in the conventional SLM scheme, which is the number of candidate sequences, is set to 16, which is equal to the number of candidate sequences that are generated by p-SLM and Class-III SLM schemes, respectively. In the proposed SLM scheme, the U' and D are set to 4 respectively in order to generate 16 candidate sequences. The figure shows that both the Class-III SLM scheme and the proposed SLM schemes can greatly decrease the computational complexity. The proposed SLM scheme can reduce complexity better compared with the Class-III SLM scheme. Table 5.5 compares the CCRR of the proposed SLM schemes with different ways of partitioning and the Class-III SLM scheme. The number of candidate sequences in the Class-III SLM schemes is denoted as U. The CCRR performance of three schemes: p-SLM, Class-III SLM, and CSLM with the same and different number of candidate sequences are compared, respectively. As it be concluded from the table, even the number of candidate sequences in the p-SLM is doubled, the computational complexity reduction is still significant. The reduction in complex multiplications is 77.8% and the reduction in complex additions is 42.8%, respectively.

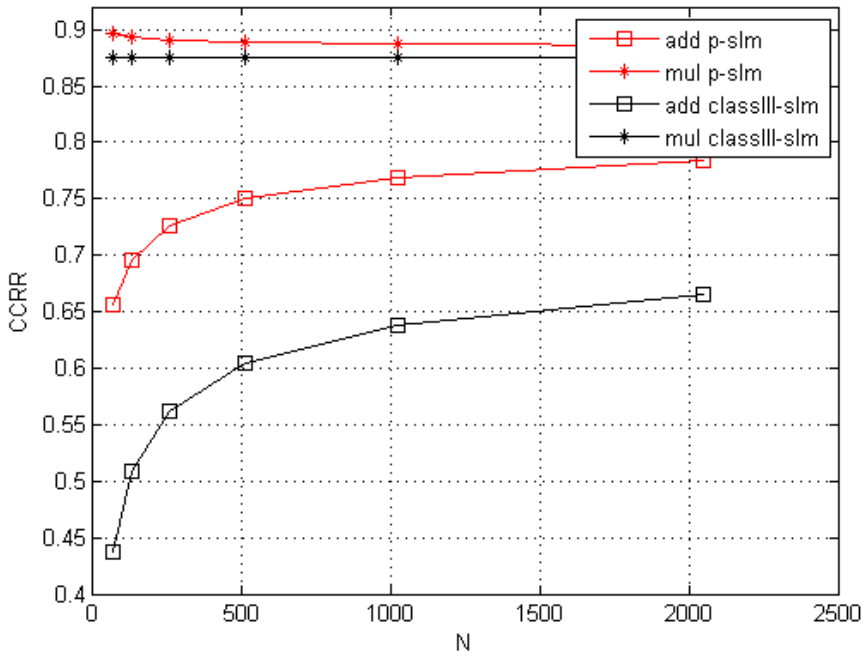

Fig. 5.15: CCRR performance of the proposed scheme.

5.4.3 Simulation results

According to the last section, the basis of the proposed work has been introduced. In this part, the simulation results are obtained for the proposed SLM, the conventional SLM, whose phase rotation is randomly taken from $\{+1 - 1\}$ and the Class-III SLM scheme with optimal cyclic shift value in Ref. [57]. The number of subcarriers that the OFDM symbols used are N=128. The number of cyclic shift values is $U = 16$ for Class-III SLM scheme and $U' = 4$ for the proposed SLM scheme, respectively, and $D = 4$ which means there are 4 different 16QAM signals can be constructed and 16 candidate sequences can be obtained totally. It should be noted that the maximum number of candidate sequences is $N/8 = 16$ in the Class-III SLM scheme without considering the phase rotation process [20] [57], and $8N/8 = 128$ in the proposed SLM scheme when the number of subcarriers $N = 128$, 16 candidate sequences are used to compare the PAPR reduction performance in order to have a fair comparison. In the results, the conventional SLM denotes as "c-SLM", the proposed SLM denotes

as "p-SLM", and Class-III SLM is "cl3-SLM".

Fig. 5.16 indicates the PAPR reduction performance with 128 subcarriers, and the number of candidate sequences in the C-SLM, Cl3-SLM, and P-SLM is 4, 16, 16, respectively. As seen from the simulation results, the PAPR reduction performance of ClassIII-SLM and p-SLM are similar. When the probability of CCDF equals to 10^{-3}, the required PAPR of original signal is over 10dB which is large. For the proposed SLM and the C-SLM, 7.3dB and 8.3dB is required, respectively. In this case, the PAPR reduction performance of the p-SLM is more effective than that of the C-SLM and also, the p-SLM requires only 2 IFFT while C-SLM requires 4 IFFT to generate 4 candidate sequences. Although the p-SLM scheme is similar as that of Class-III SLM, the computational complexity of the proposed SLM scheme is lower than that of the Class-III SLM scheme according to the last section. Moreover, the proposed SLM scheme can generate more candidate sequences while the Class-III SLM can generate 16 candidate sequences at most when no phase rotation process is applied for both SLM schemes [57].

Fig. 5.17 shows the PAPR reduction performance with 128 carriers, where the number of candidates in the C-SLM, cl3-SLM, and p-SLM are 8, 16, 16, respectively. It is seen from the simulation results that the performance of the p-SLM is similar to the performance of the Class-III SLM. Meanwhile, both of these schemes outperform the C-SLM. Moreover, the C-SLM requires 8 IFFT operations, which is a significant burden to the system.

Fig. 5.18 shows the PAPR reduction performance with 128 carriers. The number of candidates in the conventional SLM is 16, which is equal to the number of candidate sequences in the proposed SLM scheme and the Class-III SLM scheme. It is seen from the simulation results that for the same number of candidate sequences, the conventional SLM scheme has the best performance. However, the computational complexity of the proposed SLM scheme is lower that that of the Class-III SLM

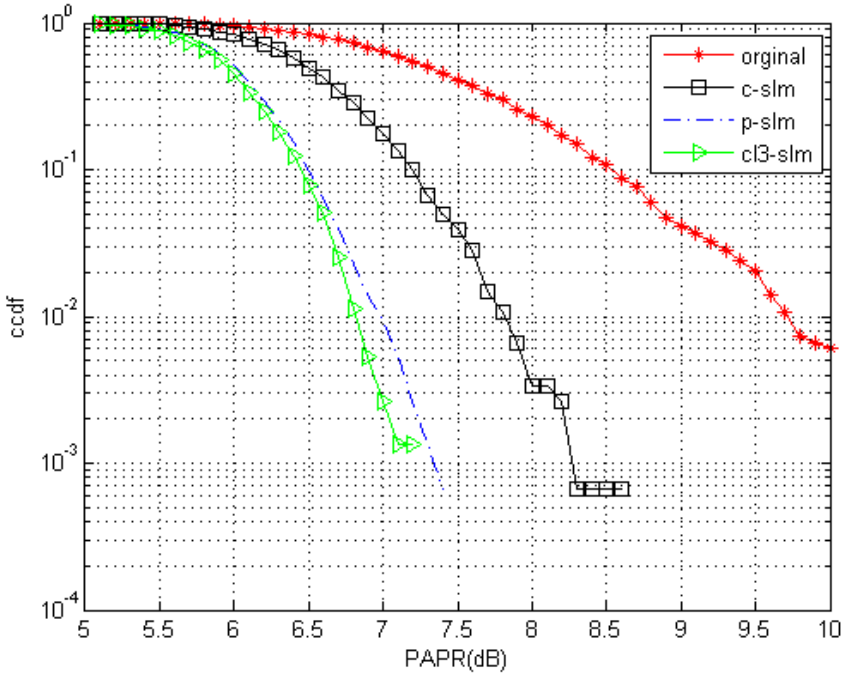

Fig. 5.16: CCDF performance comparison among three SLM schemes, 4 candidates in C-SLM.

scheme. For CCDF = 10^{-3}, the conventional SLM requires 6.8 dB, which is really low that costs 16 IFFT operations. The p-SLM is only 0.2 dB worse than the C-SLM; however the p-SLM only needs 2 IFFT operations and has the lowest computational complexity. The Class-III SLM is the second best scheme in terms of complexity reduction.

Fig. 5.19 shows the PAPR reduction performance with 256 carriers and the other conditions are the same as that in Fig. 5.18. The results are similar to the results in as Fig. 5.18, although all schemes require larger PAPR to satisfy the same CCDR requirement in Fig. 5.18.

It should be noted that although the maximum number of candidate sequences in the Class-III SLM scheme and the proposed SLM scheme is $N/8$ and N, respectively, the maximum number of candidate sequences in both Class-III SLM scheme and the proposed SLM scheme are fixed to 16, ($U' = D = 4$) in the simulations. However, it

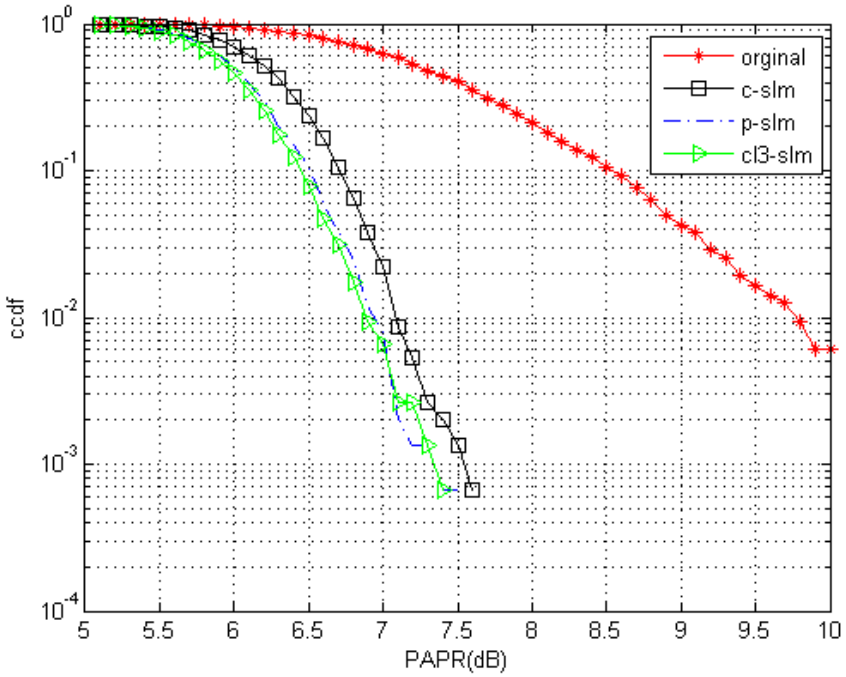

Fig. 5.17: CCDF performance comparison among three SLM schemes, 8 candidates in C-SLM.

can be expected that more candidate sequences will increase the probability of finding lower PAPR sequences which means better PAPR reduction performance. Hence, the proposed SLM scheme is more attractive than the ClassIII-SLM scheme because it can generate more candidate sequences with lower computational complexity.

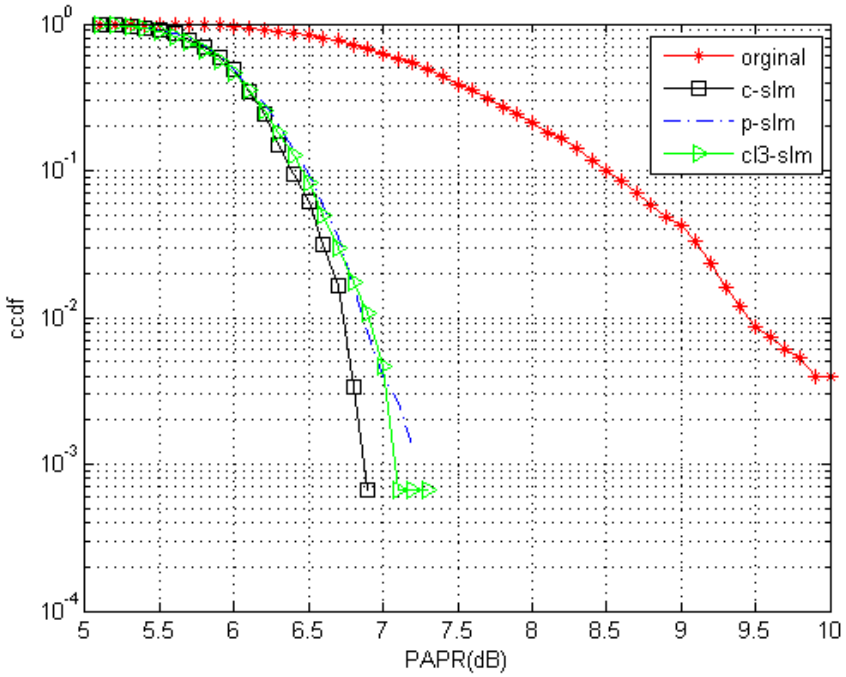

Fig. 5.18: CCDF performance comparison among three SLM schemes, 16 candidates in C-SLM.

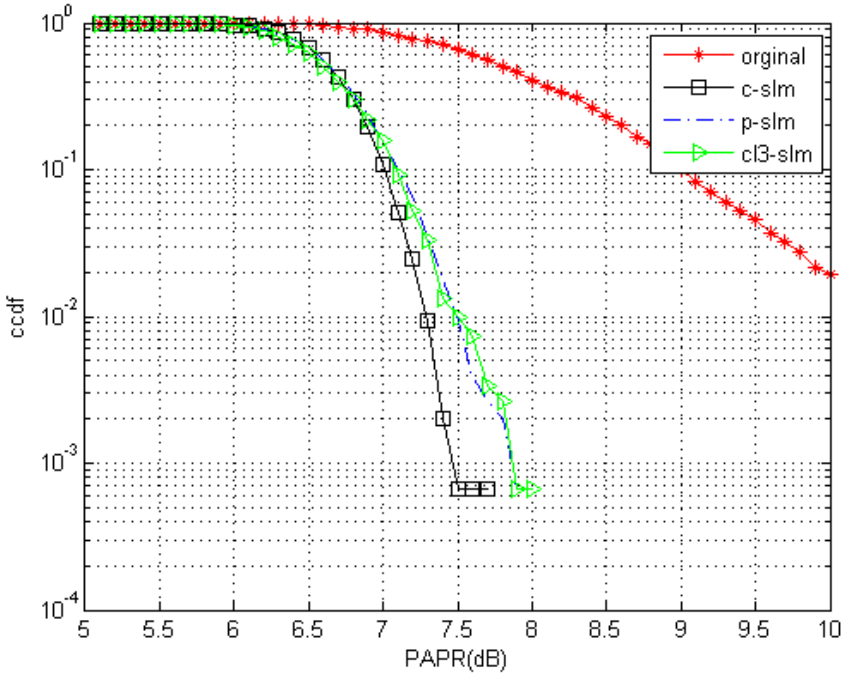

Fig. 5.19: CCDF performance comparison among three SLM schemes, 16 candidates in C-SLM.

6 THE COMPARISON AMONG THREE PROPOSED SLM SCHEMES

In this section, three proposed low complex SLM schemes are compared in terms of computational complexity and PAPR reduction performance.

6.1 Computational complexity comparison

The computational complexity of three proposed SLM schemes along with that of the conventional SLM are given in Table 6.1. As seen from the table, the computational complexity of each scheme can be written in terms of U, U', D, and M, where U is the number of candidate sequences in C-SLM, U' and D are the number of cyclic shifts and subblocks in the corresponding SLM schemes, and M is the number of phase rotation factors for the first subblock in the PPPW-SLM scheme.

Table 6.1: Comparison of computational complexity among CSLM, p-SLM, TPPW-SLM and PPPW-SLM

type	complex multiplications	complex additions
C-SLM	$(UN/2)\log_2(N)$	$(UN)\log_2(N)$
p-SLM	$N\log_2(N/2)$	$DN + (3DU'N/2) + N\log_2(N/2)$
TPPW-SLM	$(N/D)[U'^2 + D - 1 +$ $(1/2)(U' + D - 1)\log_2(N/D)]$	$(N/D)[(U' + D - 1).$ $\log_2(N/D) + DU'^2(U' - 1)]$
PPPW-SLM	$(MN/4)\log_2(N/2) +$ $((D-1)N/2D)\log_2(N/2D)$ $+(D/4)(D-1)2^{(D-1)}$	$(MN/2)\log_2(N/2) +$ $((D-1)N/2V)\log_2(N/2D) +$ $[(1 + D/4)N + MN]2^{(D-1)}$

The CCRR of the three proposed SLM schemes over the conventional SLM schemes is given by Table 6.2. In order to a have fair comparison, the number of candidate sequences is same among different SLM schemes, and the number of subcarriers is 128.

From Table 6.2, it can be see that all three proposed SLM schemes can effectively decrease the computational complexity compared with the conventional SLM scheme.

Table 6.2: CCRR of the three proposed SLM schemes when $N = 128$.

Type	complex multiplications	complex additions	$CCRR^{+}$	$CCRR^{*}$
p-SLM	768	4253	88.9%	70.3%
TPPW-SLM	800	3973	88.8%	72.2%
PPPW-SLM	1354	4721	81.2%	66.3%

The TPPW-SLM scheme can achieve 88.8% complex multiplications reduction and 72.2% complex additions reduction, which is the lowest complex SLM scheme among these proposed SLM schemes. The third proposed SLM scheme can achieve 88.9% complex multiplications reduction and 70.3% complex additions reduction, which is the second effective SLM scheme in terms of complexity reduction. Although the PPPW-SLM scheme is the last effective SLM scheme in terms of computational complexity reduction among the three proposed SLM schemes, it can still reduce around 70% computational complexity compared with the conventional SLM scheme.

6.2 PAPR reduction performance comparison

The three proposed modified SLM schemes have different performance in terms of PAPR reduction, which can be evaluated by CCDF. The CCDF performance of the three proposed SLM schemes, which have the same number of candidate sequences, is illustrated in Fig. 6.1:

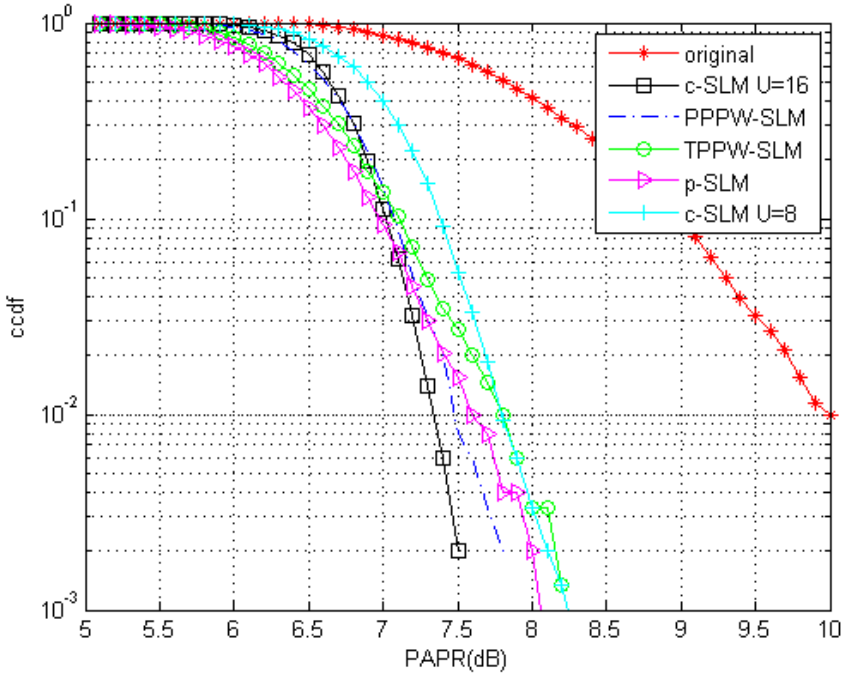

Fig. 6.1: CCDF of the three proposed SLM schemes with the same number of candidate sequences.

It is seen from the figure that for the same number of candidate sequences, the PAPR reduction performances of all the three proposed SLM scheme are worse than that of the conventional SLM scheme, which is the cost of the computational complexity reduction. The PPPW-SLM scheme has the best PAPR reduction performance among the three proposed SLM scheme. The third proposed SLM schemes is the second best in terms of PAPR reduction performance, while the TPPW-SLM scheme has the worst PAPR reduction performance.

It is known from the PAPR reduction performance comparison and computational complexity comparison that all three proposed modified SLM schemes can greatly decrease the computational complexity while keeping effective PAPR reduction performances compared with that of the conventional SLM scheme. The PPPW-SLM scheme has the best PAPR reduction performance while it has the highest complexity among the proposed SLM schemes. The third proposed SLM has the second lowest

complexity; however, its PAPR reduction performance is not as good as that of PPPW-SLM. Moreover, the TPPW-SLM scheme has the lowest complexity though it has the least PAPR reduction compared with the other two SLM schemes. Therefore, it is hard to say which one is the best.

Finally, the choice among these three proposed PAPR reduction schemes becomes a trade-off between complexity and PAPR reduction performance.

7 CONCLUSIONS AND FUTURE WORKS

7.1 Overview

In this thesis, the problem of high peak-to-average-power ratio (PAPR) in orthogonal frequency division multiplexing (OFDM) systems has been reviewed and three new PAPR reduction schemes with very low complexity have been proposed. All the proposed schemes can be considered as low-complex modified versions of the conventional selected mapping (SLM) scheme, which can significantly reduce high PAPR of OFDM signals with no distortion.

In Chapter 2, some background knowledge about OFDM systems have been presented. The OFDM system has many advantages, such as high band efficiency, robustness for multipath fading, and simple implementation by using the IFFT/FFT. However, the OFDM system also suffer some drawbacks. Among them, high PAPR is an urgent issue, which can cause signal distortion and BER depredation. In order to solve this issue, many schemes have been proposed to migrate high PAPR.

In Chapter 3, some existing PAPR reduction techniques have been reviewed. Most PAPR reduction techniques can be generally classified into three categories. The multiplicative PAPR reduction techniques includes SLM and PTS schemes. The additive PAPR reduction techniques includes clipping, TI, TR, and so on. Moreover, coding is another way for PAPR reduction, which is neither multiplicative way nor additive way. According to the comparison in Chapter 3, it is known that there is no single best PAPR reduction technique. In practice, the choice among different PAPR reduction schemes becomes a trade-off between complexity and PAPR reduction performance. Among those PAPR reduction techniques, the thesis is concentrated on the SLM scheme, which has a number of advantages, but also has comparatively high computational complexity. In order to decrease the high complexity of the SLM scheme, many modified SLM schemes have been proposed, which have been introduced in

Chapter 4.

In Chapter 4, some modified SLM schemes are reviewed. The aims of modified SLM schemes are based on two main directions. The one is to improve the PAPR reduction performance without increasing too much computational complexity, and another is to decrease the computational complexity by sacrificing some PAPR reduction performances.

In Chapter 5, three low complex SLM schemes have been proposed based on existing modified PAPR reduction techniques. The TPPW-SLM scheme is based on PPW-SLM, proposed in 2013 [54]. In the TPPW-SLM scheme, the conventional phase rotation process is replaced by the circular convolution and circular shift process in the time domain, which is a part of the Class-III SLM scheme, proposed in 2015 [57]. By using circular convolution with optimal shift values, the TPPW-SLM scheme can keep effective PAPR reduction performance and significantly reduce computational complexity. Based on the PPW-SLM scheme , the PPPW-SLM scheme has been proposed by exploiting the advantages of the PTS. However, the conventional PTS also suffers from high complexity as SLM because it requires an exhaustive search during phase optimization. In the PPPW-SLM scheme, the complexity of phase optimization is greatly decreased by introducing a low complex PTS scheme that is proposed in 2011 [44]. Simulation results show that the PPPW-SLM scheme can achieve a similar PAPR reduction performance compared with the conventional SLM scheme by reducing computational complexity by 70%. At last, a novel SLM scheme based on the the Class-III SLM scheme has been proposed. The Class-III SLM scheme that uses the optimal shift value can generate at most $N/8$ candidate sequences; however, in the proposed SLM scheme, N candidate sequences can be generated by combining a 16-QAM signal construction process [55] after the IFFT operation. The 16-QAM signal construction process can generate at most 8 different 16-QAM signals by forming 2 lower-order QPSK signals. The proposed SLM scheme can generate

more candidate sequences and lower complexity than that of Class-III and also achieve effective PAPR reduction performance.

In Chapter 6, the three proposed low complex SLM schemes are compared in terms of computational complexity reduction and PAPR reduction performance. It can be shown from the simulation results that the PPPW-SLM has the best PAPR reduction performance while the computational complexity of the PPPW-SLM is the highest among the three proposed SLM schemes. The third proposed SLMhas the second lowest computational complexity and the second best PAPR reduction performance. The TPPW-SLM is the best SLM schemes in terms of computational complexity though its PAPR reduction performance is the worst among these three proposed PAPR reduction schemes. Therefore, the choice among these three proposed PAPR reduction schemes becomes a trade-of between complexity and PAPR reduction performance.

7.2 Suggestions for future studies

The research on PAPR reduction techniques for OFDM systems performed in this thesis leads to some suggestions for the following future research.

- This thesis has focused only on some modified SLM schemes. However, there are many different kinds of PAPR reduction techniques, which have different advantages and disadvantages. In a future study, more different PAPR reduction techniques such as clipping, coding can be combined. Even in this thesis, the PPPW-SLM scheme has been proposed that is a combination of the SLM and PTS schemes. New schemes can be designed by combining different PAPR reduction techniques in order to achieve better PAPR reduction performance or lower complexity.

- In practice, OFDM can be used with conjunction with multiple-input multiple-

output (MIMO) techniques. In MIMO channels, the complexity of PAPR reduction techniques can be much higher, especially for the techniques that are based on probability, such as SLM and PTS. Applying existing PAPR reduction techniques to MIMO-OFDM is a very challenging problem.

- Most of existing PAPR reduction techniques have been proposed for single-user OFDM systems. However, OFDM can be used as multiaccess scheme, where different tones are partitioned among multiple users. This scheme is referred to as *orthogonal frequency division multiple access* (OFDMA) and is exploited in most current cellular networks. Hence, the issue of high PAPR in OFDMA systems can open up many new interesting avenues for research.

- Lastly, the current research on the SLM scheme has been mainly about how to reduce complexity of the SLM scheme. However, the SLM scheme requires the side information for each OFDM symbol in order to recover the original data information with no error at the receiver terminal. It must be noted that transmitting side information decreases throughput. In addition, false side information detection degrades the BER performance of the system drastically. Therefore, in most practical system, it is very desirable to have SLM or PTS schemes that do not require any side information.

REFERENCES

[1] T. S. Rappaport, *Wireless communications principles and practice*, 2nd ed. Prentice Hall PTR, 2002.

[2] P. B. C. A. Bruce Carlson, *Communication Systems: An Introduction to Signals and Noise in Electrical Communication, Fifth Edition*, 5th ed. McGraw-Hill Higher Education, 2009.

[3] R. G. R. Chang, "A theoretical study of performance of orthogonal multiplexing data transmission scheme," *IEEE Transactions on Communication Technology*, vol. 16, no. 4, pp. 529–540, 1968.

[4] B. Saltzberg, "Performance of an efficient parallel data transmission system," *IEEE Transactions on Communication Technology*, vol. 15, no. 6, pp. 805–811, 1967.

[5] R. W. Chang, "Orthogonal Frequency Division Multiplexing," U.S. Patent 3 488 445, Jan, 1970.

[6] P. M. E. S. B. Weinstein, "Data Transmission by Frequency-Division Multiplexing Using the Discrete Fourier Transform," *IEEE Transactions on Communication*, vol. 19, no. 5, pp. 628–634, 1971.

[7] A. Peled and A. Ruiz, "Frequency domain data transmission using reduced computational complexity algorithms," in *Acoustics, Speech, and Signal Processing, IEEE International Conference on ICASSP'80.*, vol. 5. IEEE, 1980, pp. 964–967.

[8] "Digital Vedio Broadcasting (DVB); Framing Structure, Channel Coding and Modulation for Digital Terrestrial Television," *ETSI EN 300 744 V1.4.1 ETSI*, Jan 2001.

[9] J. M. C. J. S. Chow, J. C. Tu, "A Discrete Multitone Transceiver System for HDSL Applications," *IEEE Journal on Selected Areas in Communications*, vol. 9, no. 6, pp. 895–908, 1991.

[10] J. M. C. P. S. Chow, J. C. Tu, "Performance Evaluation of a Multichannel Transceiver System for ADSL and VHDSL Services," *IEEE Journal on Selected Areas in Communications*, vol. 9, no. 6, pp. 909–919, 1991.

[11] "IEEE Standard for Local and Metropolitan Area Networks-Part 11: Wireless LAN Medium Access Control(MAC) and Physical Layer (PHY) Specifications," *IEEE Std 802.11 IEEE*, Aug 1999.

[12] "IEEE Standard for Local and Metropolitan Area Networks-Part 16: Air Interface for Fixed Broadband Wireless Access Systems," *IEEE Std 802.16-2004 IEEE*, Oct 2004.

[13] "IEEE Standard for Local and Metropolitan Area Networks-Part 16: Air Interface for Fixed Broadband Wireless Access Systems-Amendment 2:Physical and Medium Access Control Layer for Combined Fixed and Mobile Operation in Licensed Bands," *IEEE Std 802.16e-2005 IEEE*, Feb 2006.

[14] K. Z. W. B. Wang, *Wideband Wireless Communication OFDM Technologies*, 1st ed. Posts and Telecom Press, 2003.

[15] D.-W. Lim, S.-J. Heo, and J.-S. No, "An overview of peak-to-average power ratio reduction schemes for ofdm signals," *Communications and Networks, Journal of*, vol. 11, no. 3, pp. 229–239, 2009.

[16] S. G. Lee, "Performance of concatenated fec under fading channel in wireless-man ofdm system," in *Advanced Information Networking and Applications, 2005. AINA 2005. 19th International Conference on*, vol. 1. IEEE, 2005, pp. 781–785.

[17] S. V. Vaseghi, *Advanced digital signal processing and noise reduction.* John Wiley & Sons, 2008.

[18] R. W. S. A. V. Oppenheim and J. R. Buck, *Discrete-Time Signal Processing.* Upper Saddle River, NJ: Prentice-Hall, 1998.

[19] W. Y. Zou and Y. Wu, "Cofdm: An overview," *Broadcasting, IEEE Transactions on*, vol. 41, no. 1, pp. 1–8, 1995.

[20] C.-P. Li, S.-H. Wang, and C.-L. Wang, "Novel low-complexity slm schemes for papr reduction in ofdm systems," *Signal Processing, IEEE Transactions on*, vol. 58, no. 5, pp. 2916–2921, 2010.

[21] H.-B. Jeon, K.-H. Kim, J.-S. No, and D.-J. Shin, "Bit-based slm schemes for papr reduction in qam modulated ofdm signals," *Broadcasting, IEEE Transactions on*, vol. 55, no. 3, pp. 679–685, 2009.

[22] V. Kulkarni and A. Bhalchandra, "An overview of various techniques to reduce the peak-to-average power ratio in multicarrier transmission systems," in *Computational Intelligence & Computing Research (ICCIC), 2012 IEEE International Conference on.* IEEE, 2012, pp. 1–5.

[23] S. H. Han and J. H. Lee, "An overview of peak-to-average power ratio reduction techniques for multicarrier transmission," *Wireless Communications, IEEE*, vol. 12, no. 2, pp. 56–65, 2005.

[24] R. W. Bäuml, R. F. Fischer, and J. B. Huber, "Reducing the peak-to-average power ratio of multicarrier modulation by selected mapping," *Electronics Letters*, vol. 32, no. 22, pp. 2056–2057, 1996.

[25] S. H. Müller, R. W. Bäuml, R. F. Fischer, and J. B. Huber, "Ofdm with reduced peak-to-average power ratio by multiple signal representation," in *Annales des télécommunications*, vol. 52, no. 1-2. Springer, 1997, pp. 58–67.

[26] J. Tellado, *Multicarrier modulation with low PAR: applications to DSL and wireless*. Springer Science & Business Media, 2006, vol. 587.

[27] R. O'Neill and L. Lopes, "Envelope variations and spectral splatter in clipped multicarrier signals," in *Personal, Indoor and Mobile Radio Communications, 1995. PIMRC'95. Wireless: Merging onto the Information Superhighway., Sixth IEEE International Symposium on*, vol. 1. IEEE, 1995, pp. 71–75.

[28] H. Ochiai and H. Imai, "Performance of the deliberate clipping with adaptive symbol selection for strictly band-limited ofdm systems," *Selected Areas in Communications, IEEE Journal on*, vol. 18, no. 11, pp. 2270–2277, 2000.

[29] N. Benvenuto, R. Dinis, D. Falconer, and S. Tomasin, "Single carrier modulation with nonlinear frequency domain equalization: an idea whose time has comeagain," *Proceedings of the IEEE*, vol. 98, no. 1, pp. 69–96, 2010.

[30] C. Ciochina and H. Sari, "A review of ofdma and single-carrier fdma," in *Wireless Conference (EW), 2010 European*. IEEE, 2010, pp. 706–710.

[31] S. H. Han and J. H. Lee, "An overview of peak-to-average power ratio reduction techniques for multicarrier transmission," *Wireless Communications, IEEE*, vol. 12, no. 2, pp. 56–65, 2005.

[32] V. Vijayarangan and R. Sukanesh, "An overview of techniques for reducing peak to average power ratio and its selection criteria for orthogonal frequency division multiplexing radio systems," *Journal of theoretical and applied information technology*, vol. 5, no. 1, pp. 25–36, 2009.

[33] C.-L. Wang, S.-J. Ku, and C.-J. Yang, "A low-complexity papr estimation scheme for ofdm signals and its application to slm-based papr reduction," *Selected Topics in Signal Processing, IEEE Journal of*, vol. 4, no. 3, pp. 637–645, 2010.

[34] E. O. Brigham, "The {F} ast {F} ourier {T} ransform and its applications," 1988.

[35] J. Armstrong, "Peak-to-average power reduction for ofdm by repeated clipping and frequency domain filtering," *Electronics letters*, vol. 38, no. 5, pp. 246–247, 2002.

[36] X. Li and L. J. Cimini Jr, "Effects of clipping and filtering on the performance of ofdm," in *Vehicular Technology Conference, 1997, IEEE 47th*, vol. 3. IEEE, 1997, pp. 1634–1638.

[37] M. G. Parker and C. Tellambura, "Golay-davis-jedwab complementary sequences and rudin-shapiro constructions," in *International Symposium in Information Theory*, 2001, p. 302.

[38] L. Wang and C. Tellambura, "A clipping guided sigh-selection algorithm for papr reduction ofdm systmes," *Trans. Signal Process. IEEE*, vol. 56, no. 11, pp. 5644–5653, 2008.

[39] Y. Wang, L.-H. Wang, J.-H. Ge, and B. Ai, "Nonlinear companding transform technique for reducing papr of odfm signals," *Consumer Electronics, IEEE Transactions on*, vol. 58, no. 3, pp. 752–757, 2012.

[40] N. Chaudhary and L. Cao, "Non-symmetric decompanding for improved performance of companded ofdm systems," *Wireless Communications, IEEE Transactions on*, vol. 6, no. 8, pp. 2803–2806, 2007.

[41] A. E. Jones, T. A. Wilkinson, and S. Barton, "Block coding scheme for reduction of peak to mean envelope power ratio of multicarrier transmission schemes," *Electronics letters*, vol. 30, no. 25, pp. 2098–2099, 1994.

[42] R. D. Van Nee, "Ofdm codes for peak-to-average power reduction and error correction," in *Global Telecommunications Conference, 1996. GLOBECOM'96.'Communications: The Key to Global Prosperity*, vol. 1. IEEE, 1996, pp. 740–744.

[43] C. Schurgers, "Systematic approach to peak-to-average power ratio in ofdm," in *International Symposium on Optical Science and Technology*. International Society for Optics and Photonics, 2001, pp. 454–464.

[44] L. Wang and J. Liu, "Papr reduction of ofdm signals by pts with grouping and recursive phase weighting methods," *Broadcasting, IEEE Transactions on*, vol. 57, no. 2, pp. 299–306, 2011.

[45] R. J. Baxley and T. G. Zhou, "Comparing selected mapping and partial transmit sequence for par reduction," *Broadcasting, IEEE transactions on*, vol. 53, no. 4, pp. 797–803, 2007.

[46] S.-B. Ryu, S.-K. Kim, and R. Sang-Burm, "Interleaving method without side information for the papr reduction of ofdm system," in *Communications and Information Technologies, 2007. ISCIT'07. International Symposium on*. IEEE, 2007, pp. 72–76.

[47] S. O'Hara, B. Chen, and J. Periard, "A bandwidth efficient peak power reduction scheme for multicarrier modulation using selected mapping," in *Proc. Conference on Information Sciences and Systems*, 2003.

[48] T. Jiang and Y. Wu, "peak to average power ratio reduction in ofdm systems," *IEEE transactions on broadcasting*, vol. 54, no. 2, 2008.

[49] Y. Wang, W. Chen, and C. Tellambura, "Genetic algorithm based nearly optimal peak reduction tone set selection for adaptive amplitude clipping papr reduction," *Broadcasting, IEEE Transactions on*, vol. 58, no. 3, pp. 462–471, 2012.

[50] L. Guan and A. Zhu, "Gaussian pulse-based two-threshold parallel scaling tone reservation for papr reduction of ofdm signals," *International Journal of Digital Multimedia Broadcasting*, vol. 2011, 2011.

[51] A. D. S. Jayalath and C. Tellambura, "The use of interleaving to reduce the peak-to-average power ratio of an ofdm signal," in *Global Telecommunications Conference, 2000. GLOBECOM'00. IEEE*, vol. 1. IEEE, 2000, pp. 82–86.

[52] M. García, J. M. Páez-Borrallo, and O. Edfors, "Orthogonal pilot sequences for peak-to-average power reduction in ofdm," in *Vehicular Technology Conference, 2001. VTC 2001 Fall. IEEE VTS 54th*, vol. 2. IEEE, 2001, pp. 650–654.

[53] C. Tellambura, "Use of m-sequences for ofdm peak-to-average power ratio reduction," *Electronics Letters*, vol. 33, no. 15, pp. 1300–1301, 1997.

[54] L. Wang and J. Liu, "Partial phase weighting selected mapping scheme for peak-to-average power ratio reduction in orthogonal frequency division multiplexing system," *IET Communications*, vol. 9, no. 2, pp. 147–155, 2014.

[55] L. Yang, Y.-M. Siu, K.-K. Soo, and S.-Q. Li, "New construction scheme to reduce the papr of m-qam ofdm signal," *Wireless Personal Communications*, vol. 80, no. 3, pp. 1217–1230, 2015.

[56] P. Cheng, Y. Xiao, L. Dan, and S. Li, "Improved slm for papr reduction in ofdm system," in *Personal, Indoor and Mobile Radio Communications, 2007. PIMRC 2007. IEEE 18th International Symposium on.* IEEE, 2007, pp. 1–5.

[57] J.-Y. Woo, H.-S. Joo, K.-H. Kim, J.-S. No, and D.-J. Shin, "Papr analysis of class-iii slm scheme based on variance of correlation of alternative ofdm signal sequences."

[58] C.-L. Wang and Y. Ouyang, "Low-complexity selected mapping schemes for peak-to-average power ratio reduction in ofdm systems," *Signal Processing, IEEE Transactions on*, vol. 53, no. 12, pp. 4652–4660, 2005.

[59] C.-L. Wang, S.-S. Wang, and H.-L. Chang, "A low-complexity slm based papr reduction scheme for sfbc mimo-ofdm systems," in *Wireless Communications and Networking Conference (WCNC), 2011 IEEE*. IEEE, 2011, pp. 1449–1453.

[60] G. Lu, P. Wu, and C. Carlemalm-Logothetis, "Peak-to-average power ratio reduction in ofdm based on transformation of partial transmit sequences," *Electronics Letters*, vol. 42, no. 2, pp. 105–106, 2006.

VITA AUCTORIS

NAME:	Siyu Zhang
PLACE OF BIRTH:	Beijing, China
YEAR OF BIRTH:	1992
EDUCATION:	Jilin University, Changchun, Jilin, China Bachelor of Electrical Engineering, Communication Engineering 2010-2014
	University of Windsor, Windsor ON, Canada Master of Applied Science, Electrical and Computer Engineering 2014-2016